A Combined CDMA/SCM/WDM Communication System

A Thesis submitted

in partial fulfilment of the requirement

for the degree of
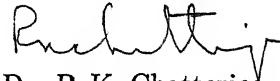
MASTER OF TECHNOLOGY

by
Suman Lata Shukla

to the

Department of Electrical Engineering
Indian Institute of Technology Kanpur

December 1995

CERTIFICATE

It is certified that the work contained in this thesis titled "**A Combined CDMA/ SCM/WDM Communication System**" by **Suman Lata Shukla** has been carried out under my supervision and that this work has not been submitted elsewhere for a degree.
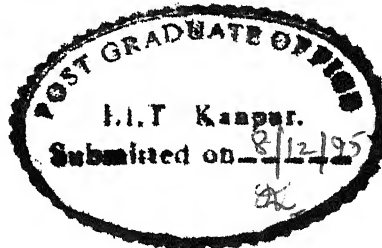
Dr. P. K. Chatterjee
Professor
Dept. of Electrical Engineering
I. I. T. Kanpur.

December 8, 1995.

POST GRADUATE OFFICE
I.I.T Kanpur.
Submitted on 8/12/95

EE-1995- M-SHU-COM

Abstract

A multichannel CDMA/SCM/WDM system has been studied where several optical carriers are wavelength division multiplexed (WDM), and each such carrier is modulated by eight multiplexed microwave subcarriers received through line-of-sight free space links. The subcarriers are modulated in BPSK or QPSK by the spread-spectrum sequences. Both phase modulation/coherent detection and intensity modulation/direct detection schemes have been studied for the fiber optic link. Different code sequence lengths, N=127, 255 and 511, have been used. Microwave bands of 2-18 GHz and 26-30 GHz have been considered for free space transmission. Signal-to-noise ratio and probability of error (Pe) have been calculated for different sequence lengths, number of sequences K, and input signal power P_s. The effects of thermal noise, shot noise, intermodulation noise and multiple-access interference have been considered for these calculations. $Pe = 10^{-9}$ is obtained for N=127 and K=10 at a received signal power of -41 dBm for coherent detection. It is not possible to obtain an error probability of 10^{-9} for N=127 and K=10 using direct detection. An error floor occurs in this case at $Pe = 10^{-5}$, whereas an error floor for coherent detection occurs at $Pe = 10^{-10}$. However, in the 26-30 GHz band for direct detection $Pe = 10^{-9}$ is obtained for $P_s = -28$ dBm, N=127 and K=5. On the other hand, for coherent detection in this band $P_s = -48$ dBm is found to be adequate.

Acknowledgements

Contents

List of Figures

Chapter 1

Introduction

The most dominant consideration in the design of a communication system is the conservation of bandwidth. Therefore, the simultaneous transmission of a large number of audio/video channels demands for some form of multiple-access technique in which a number of users share a common channel bandwidth.There are three types of multiple-access techniques, frequency-division multiple-access (FDMA), time-division multiple-access (TDMA) and code-division multiple-access (CDMA). In FDMA all users share the channel at the same time, but each transmits in its own frequency band. In TDMA, the users transmit in turn in their own unique time slots. While transmitting, each user has exclusive use of the entire channel bandwidth. In CDMA, a number of users occupy all of the available transmission band all the time. CDMA does not require time (as in TDMA) or frequency (as in FDMA) coordination between the transmitters, but, it requires a large transmission bandwidth. With the advent of fiber optic channels bandwidth is no more a serious problem. Enormous bandwidth capacity of fiber optic channels can be utilized to provide a further increase in the number of channels transmitted by using subcarrier multiplexing, i.e., simultaneous transmission of a number of carriers along one communication channel using a single optical wavelength. This capacity can be further enhanced by using several optical carriers in the wavelength-division multiplexing (WDM) mode.

1.1   Code Division Multiple Access

The CDMA techniques are those multiple-access methods in which the multiple-access capability is due to coding. Each user is assigned a particular code sequence which is modulated on the carrier along with the digital data. The data from an individual transmitter can be detected and recovered only by a properly synchronized receiving station that knows the code being used. The two most common forms of CDMA are frequency-hopped (FH) CDMA and direct-sequence (DS) CDMA. In FH-CDMA, the carrier frequency varies pseudo-randomly according to the code sequence. In DS-CDMA, the carrier is phase-modulated by the digital data sequence and the code sequence. In this thesis only DS-CDMA has been considered.

The main advantages of using CDMA are:

1) Protection against externally generated interfering signals with finite power.
2) Suppression of the interference arising from other users of the channel in multiple-access communications systems.
3) Hiding a signal by transmitting it at a low power and, thus, making it difficult for an unintended listener to detect in the presence of background noise.
4) Achieving message privacy in the presence of other listeners by superimposing a pseudo-random pattern on a transmitted message.
5) Synchronization among users is not required.

1.2   Subcarrier Multiplexing

SCM is a two stage modulation technique in which various messages modulate corresponding carriers in some suitable fashion, and the multiplexed sum of these carriers in turn modulates an ultimate carrier. The carriers used in the first stage of modulation are called subcarriers. The block schematic of a general SCM system is shown in Fig. 1.1.
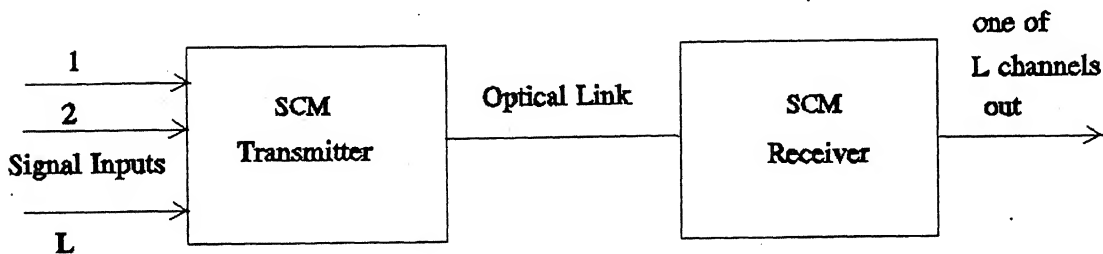
Figure 1.1: Block schematic of a general SCM system

The main advantages of using SCM are:

1) SCM enables one to multiplex a number of analog and/or digital signals either optically or electronically.
2) It allows one to take advantage of the large bandwidth available with lasers and detectors.
3) SCM provides improved receiver sensitivity which implies increase in the number of users for network environment and increase in the repeater distance for point to

point links.

4) Finally, in SCM each channel is continuously available and independent of all other channels and there is no need for synchronization between each channel.

SCM has some disadvantages also which are:

1) In SCM, as the baseband signal consists of a number of channels having equally distant centre frequencies, adjacent channel interference may arise. This interference can be limited by a proper selection of the centre frequencies.

2) Intermodulation distortion (IMD) is generated because of the non-linearity in the transmission system. This is true for both direct detection and coherent systems. In the case of intensity-modulated/direct-detection systems, IMD is mainly generated at the transmitter. In coherent SCM systems, IMD is mainly generated at the receiver.

3) The algebraic addition of L microwave signals at different frequencies requires that if severe intermodulation distortion is to be avoided, the power radiated at each microwave subcarrier must be less than $\frac{1}{\sqrt{L}}$ of the laser's peak power, a serious link budget penalty.

1.3 Wavelength Division Multiplexing
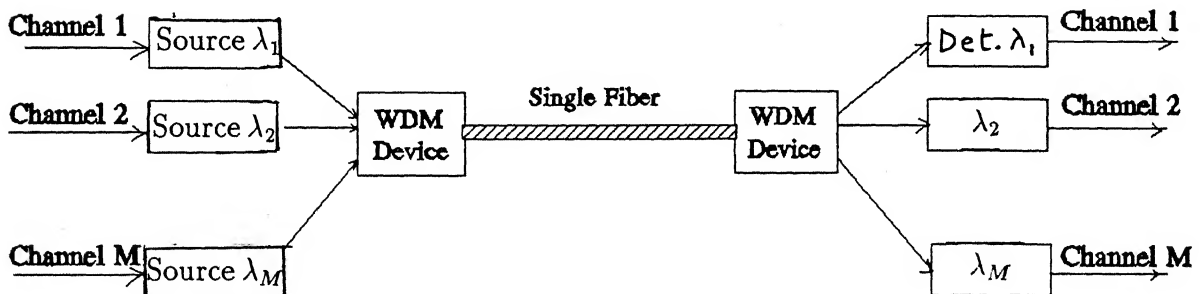
Figure 1.2: Block schematic of a general WDM system

In WDM, optical signals from many different light sources having properly spaced peak emission wavelengths are transmitted simultaneously over the same fiber. By operating each source at a different peak wavelength, the integrity of the independent

messages from each source is maintained for subsequent conversion to electrical signals at the receiving end. The block schematic of a general WDM system is shown in Fig. 1.2. The fundamental reason for the superiority of WDM is that the full optical power of a laser is available for each channel. For SCM, as is indicated above, avoidance of intermodulation does not allow this. The use of WDM has been found to have a disadvantage for extremely long links that require many cascaded amplifiers, because this compounds the unevenness of gain with wavelength.

1.4 Proposed CDMA and SCM Systems

In this section some CDMA and SCM systems proposed earlier have been briefly reviewed.

One of the first papers which dealt with asynchronous DS-CDMA systems was by Pursley [1]. In this paper an analysis of asynchronous biphase direct sequence spread-spectrum multiple-access (SSMA) communication system is presented. Expression for the average signal-to-noise ratio and probability of error at the receiver output have been obtained.

Garber and Pursley [2] analysed quadriphase spread-spectrum multiple-access. Two cases have been analysed, offset Q-SSMA with orthogonal biphase carriers and offset Q-SSMA with orthogonal quadriphase-coded carriers. Average SNR for the in phase and the quadrature branches are calculated.

Geraniotis [3] has analysed SSMA with FSK and DPSK as modulation schemes. Average probability of error for the systems using deterministic as well as random signature sequences has been presented. The performance of the SSMA systems using different modulation schemes like PSK, DPSK and FSK has been compared.

Interest in the SCM optical communication systems began with Darcie's paper "Subcarrier Multiplexing for Multiple-Access Light-wave Networks" [4]. The paper described the applicability of subcarrier multiplexing to lightwave multiple-access networks. Advantages and limitations of subcarrier multiplexing were demonstrated, and it was shown that SCM provided a relatively simple means of multiplexing while maintaing a high receiver sensitivity.

Desam [5], [6] analysed the effect of optical interference in lightwave subcarrier systems employing multiple optical carriers.

The first example of a system using more than one octave of bandwidth was reported by R. Olshansky and P. Hill [7]. They presented the performance results of a 20 channel SCM video distribution system over a 12 km single mode fiber link.

Gross and Olshansky considered the multichannel coherent FSK experiments using SCM techniques [8]. They considered 20 FSK channels at 100 Mbps each to be transmitted on one optical carrier using microwave subcarriers in a multi-octave configuration. The paper also presented an analysis and experimental investigation of intermodulation distortion to determine the spectral form of the second and third order distortion terms.

In a paper by M.T.Abuelma'atti [9], carrier-to-intermodulation ratio for a laser diode has been calculated using laser rate equations.

4

1.5   Present Work

Present work is an effort to analyse a combined CDMA/SCM/WDM system. data rate used is 2.048 Mbps. microwave bands of 2-6 GHz as well as 26-30 Ghz have been considered for the analysis of the system. Eight microwave subcarrier channels, each obtained by code-division multiple-access of K signals, are subcarrier multiplexed. The resulting signal modulates an optical source. The signals from different optical sources are wavelength-division multiplexed and are transmitted through a single fiber. In this scheme a user is identified by a specific subcarrier frequency and a particular code sequence. The system has been analysed using coherent as well as direct-detection at the receiver. IMD analysis has been carried out for both the cases and the method to obtain second and third order IMD is given. Adjacent channel interference and intersymbol interference are neglected. The SNR and the probability of error have been calculated. Plots showing the variation of probability of error with the received power have been given for different sequence lengths N and the number of users K.

1.6   Thesis Layout

Chapter 2 considers the effects of nonlinearity in the system transfer characteristics. It is shown that the level of second and third harmonic distortion is negligible compared to the second and third order intermodulation distortion (IMD) respectively. It is also shown that the power spectral density of IMD term can be obtained by convolving the individual signal spectra.

Chapter 3 provides an analysis of an asynchronous DS-SSMA communication system. Expressions for SNR have been given including the effects of multiple-access interference and the thermal noise.

Chapter 4 deals with the analysis of the CDMA/SCM/WDM system for the 2-6 GHz band using coherent detection of the optical carrier at the receiver. Second- and third-order IMD calculations have been done for use in this analysis.

Chapter 5 presents the CDMA/SCM/WDM system for the frequency band of 2-6 GHz, but, using direct-detection of the optical signal at the receiver.

In chapter 6 the system calculations have been given for the 26-30 GHz band.

Finally, the thesis is concluded in chapter 7.

Chapter 2

Intermodulation Noise Generation

2.1   Intermodulation

The application of a signal $e_i(t)$ to a non-linear device results in an output $e_o(t)$ consisting of components at the input frequencies and spurious components at d.c., harmonics of the applied frequency, and many additional frequency components that are various combinations of sum and difference frequencies of the input signals. These latter frequency components are reffered to as intermodulation (IM) products. The IM products increase the overall noise-level and thus result in a degradation of the transmitted signal.
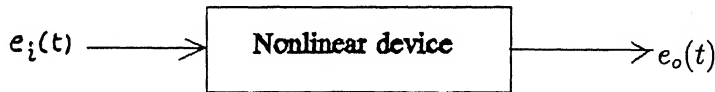
The output $e_o(t)$ in general is given by

$$e_o(t) = a_1 e_i(t) + a_2 e_i^2(t) + a_3 e_i^3(t) + \cdots \tag{2.1}$$

For all practical purposes, coefficients of fourth and higher order terms in the series are sufficiently small to be negligible, so that $e_o(t)$ can be approximated as

$$e_o(t) = a_1 e_i(t) + a_2 e_i^2(t) + a_3 e_i^3(t) \tag{2.2}$$

So we will consider only upto third order terms for analysis in this thesis.

2.2 Intermodulation Distortion For Discrete Frequency Signals

Consider that the input signal consists of three discrete frequencies, i.e.,

$$e_i(t) = A \cos 2\pi f_1 t + B \cos 2\pi f_2 t + C \cos 2\pi f_3 t \tag{2.3}$$

The output $e_o(t)$ is given by

$$
\begin{aligned}
e_o(t) =\ & a_1(A \cos 2\pi f_1 t + B \cos 2\pi f_2 t + C \cos 2\pi f_3 t) \\
& + a_2(A \cos 2\pi f_1 t + B \cos 2\pi f_2 t + C \cos 2\pi f_3 t)^2 \\
& + a_3(A \cos 2\pi f_1 t + B \cos 2\pi f_2 t + C \cos 2\pi f_3 t)^3
\end{aligned} \tag{2.4}
$$

Using trigonometric identities the output can be arranged in a table 2.1 [10].

	Term1	Term2	Term3
d.c.		$\frac{1}{2}a_2(A^2 + B^2 + C^2)$	
First order	$a_1(A\cos 2\pi f_1 t + B\cos 2\pi f_2 t$ $+ C\cos 2\pi f_3 t)$		$\frac{3}{4}a_3 A(A^2 + 2B^2 + 2C^2)\cos 2\pi f_1 t$ $+\frac{3}{4}a_3 B(B^2 + 2C^2 + 2A^2)\cos 2\pi f_2 t$ $+\frac{3}{4}a_3 C(C^2 + 2A^2 + 2B^2)\cos 2\pi f_3 t$
Second order		$\frac{1}{2}a_2(A^2\cos 4\pi f_1 t + B^2\cos 4\pi f_2 t$ $+ C^2\cos 4\pi f_3 t)$ $+ a_2 AB(\cos 2\pi(f_1 + f_2)t$ $+ \cos 2\pi(f_1 - f_2)t)$ $+ a_2 BC(\cos 2\pi(f_2 + f_3)t$ $+ \cos 2\pi(f_2 - f_3)t)$ $+ a_2 AC(\cos 2\pi(f_1 + f_3)t$ $+ \cos 2\pi(f_1 - f_3)t)$	
Third order			$\frac{1}{4}a_3(A^3\cos 6\pi f_1 t + B^3\cos 6\pi f_2 t + C^3\cos 6\pi f_3 t)$ $+\frac{3}{4}a_3 A^2 B(\cos 2\pi(2f_1 + f_2)t + \cos 2\pi(2f_1 - f_2)t)$ $+\frac{3}{4}a_3 A^2 C(\cos 2\pi(2f_1 + f_3)t + \cos 2\pi(2f_1 - f_3)t)$ $+\frac{3}{4}a_3 B^2 A(\cos 2\pi(2f_2 + f_1)t + \cos 2\pi(2f_2 - f_1)t)$ $+\frac{3}{4}a_3 B^2 C(\cos 2\pi(2f_2 + f_3)t + \cos 2\pi(2f_2 - f_3)t)$ $+\frac{3}{4}a_3 C^2 A(\cos 2\pi(2f_3 + f_1)t + \cos 2\pi(2f_3 - f_1)t)$ $+\frac{3}{4}a_3 C^2 B(\cos 2\pi(2f_3 + f_2)t + \cos 2\pi(2f_3 - f_2)t)$ $+\frac{3}{2}a_3 ABC(\cos 2\pi(f_1 + f_2 + f_3)t + \cos 2\pi(f_1 + f_2$ $+\cos 2\pi(f_1 - f_2 + f_3)t + \cos 2\pi(f_1 - f_2 - f_3)t)$

Table 2.1

It can be observed from table [2.1] that second order terms contain second harmonic $(2f_1, 2f_2, 2f_3)$ as well as IMD terms. Similarly, third order terms are made up of third harmonic as well as third order IMD terms. Third order IMD terms are again of two types. One type of terms occur due to the beating of three frequencies $(f_1 \pm f_2 \pm f_3)$, and the second type of terms occur due to the beating of second harmonic of a frequency with another $(2f_1 \pm f_2, 2f_1 \pm f_3$ etc.). In both the second order and third order terms, power level of IMD terms is higher than that of harmonic terms as shown below.

Power of a second harmonic term

$$
\begin{aligned}
P_{2f_1} &= 10 \log_{10}[(\tfrac{1}{2}a_2 A^2)^2/2] \\
&= 20 \log_{10}[\tfrac{1}{2}a_2 A^2] - 3
\end{aligned}
\tag{2.5}
$$

Power of a second order IMD term

$$
\begin{aligned}
P_{f_1 \pm f_2} &= 10 \log_{10}[(a_2 AB)^2/2] \\
&= P_{2f_1} + P_{f_2} - P_{f_1} + 6
\end{aligned}
\tag{2.6}
$$

where $P_{f_2} = 10 \log_{10}[(a_1 B)^2/2]$ and $P_{f_1} = 10 \log_{10}[(a_1 A)^2/2]$.
If A = B, $P_{f_1} = P_{f_2}$ implies

$$
P_{f_1 \pm f_2} = P_{2f_1} + 6
\tag{2.7}
$$

which shows that the second order IMD terms are higher in power level than the second harmonic terms by 6 dB.

For the case of three distinct frequencies, output contains three second harmonic terms and 6 second order IMD terms.
If we assume A = B = C,

$$
\begin{aligned}
P_{2HD} &= 10 \log 3[\tfrac{1}{2}a_2 A^2]^2/2 \\
&= 4.7 + P_{2f_1}
\end{aligned}
\tag{2.8}
$$

and total second order IMD power is

$$
\begin{aligned}
P_{2IMD} &= 10 \log_{10}[6(a_2 AB)^2/2] \\
&= 13.7 + P_{2f_1}
\end{aligned}
\tag{2.9}
$$

which shows that total power of the second order IMD terms exceeds that of the second harmonic distortion by 9 dB.

If the input signal is assumed to contain N discrete frequencies then the output signal will have N second harmonic distortion terms and $2N_{C_2} = N(N-1)$ second order IMD terms. In this general case

$$
P_{2HD} = 10 \log_{10} N + P_{2f_1}
\tag{2.10}
$$

and

$$
\begin{aligned}
P_{2IMD} &= 10 \log_{10} N(N-1) + P_{2f_1} + 6 \\
&= P_{2HD} + 10 \log_{10}(N-1) + 6
\end{aligned}
\tag{2.11}
$$

which shows that the total second order IMD power exceeds the total second harmonic distortion power by $[6 + 10 \log_{10}(N-1)]$ dB. Hence the second harmonic distortion becomes negligibly small as compared to second order IMD with large N.
Similarly, in the case of third order

$$P_{3f_1} = 20 \log_{10}[\frac{1}{4}a_3 A^3] - 3 \qquad (2.12)$$

$$P_{2f_1 \pm f_2} = P_{3f_1} + P_{f_2} - P_{f_1} + 9.54 \qquad (2.13)$$

$$P_{f_1 \pm f_2 \pm f_3} = P_{3f_1} + P_{f_2} + P_{f_3} - 2P_{f_1} + 15.56 \qquad (2.14)$$

If A = B = C,

$$P_{f_1 \pm f_2 \pm f_3} = P_{2f_1 \pm f_2} + 6 \qquad (2.15)$$

Eq. implies that the third order IMD terms of the type $(2f_1 \pm f_2)$ are one fourth (-6 dB) the power level of the $(f_1 \pm f_2 \pm f_3)$ type of terms.

When the input signal cotains N discrete frequencies,the output signal will have N third harmonic distortion terms. As N becomes large, third order IMD terms are dominated by the terms of the type $(f_1 \pm f_2 \pm f_3)$ and increases as N^3 [4]. By reasoning similar to that used for second order terms, it can be said that the third harmonic distortion becomes negligibly small as compared to third order IMD with large N. A signal having continuous spectrum can be considered as the summation of very large number of infinitesimally distant discrete frequencies. Hence, in this case also, harmonic distortion is negligible compared to the IMD for both second and third order terms.

2.3   IMD For Bandlimited Random Signals

In case, the input signal $e_i(t)$ to the nonlinear device is a multiplexed signal, the intermodulation noise can be computed using spectral densities and autocorrelation functions [10]. From (3.1), the output is given by

$$e_o(t) = a_1 e_i(t) + a_2 e_i^2(t) + a_3 e_i^3(t) \qquad (2.16)$$

If $S_1(f)$ is the power spectral density of the bandlimited signal $e_i(t)$, the desired spectrum at the output will be $a_1^2 S_1(f)$. The spectrum at the output corresponding to the $e_i^2(t)$ term will correspond to all of the second order intermodulation noise and will be denoted by $a_2^2 S_2(f)$. Similarly, third order intermodulation noise due to $e_i^3(t)$ will be denoted by $a_3^2 S_3(f)$.

$S_2(f)$ and $S_3(f)$ can be determined by the use of autocorrelation functions. Appendix A shows that if $e_i(t)$ is assumed to be Gaussian, the autocorrelation (ACF) of $e_i^2(t)$ and $e_i^3(t)$ can be written in terms of the autocorrelation function $R_1(\tau)$ of $e_i(t)$. The autocorrelation function $R_2(\tau)$ of $e_i^2(t)$ is given by

$$R_2(\tau) = 2R_1^2(\tau) + R_1^2(0) \qquad (2.17)$$

and, the autocorrelation function $R_3(\tau)$ of $e_i^3(t)$ is given as

$$R_3(\tau) = 9R_1(\tau)R_1^2(0) + 6R_1^3(\tau) \qquad \cdot \qquad (2.18)$$

The PSD of $e_i^2(t)$ is

$$
\begin{aligned}
S_2(f) &= \int_{-\infty}^{\infty} R_2(\tau)e^{-j2\pi f\tau}d\tau \\
&= \int_{-\infty}^{\infty} [2R_1^2(\tau) + R_1^2(0)]e^{-j2\pi f\tau}d\tau \\
&= [\int_{-\infty}^{\infty} S_1(f)\,df]^2\delta(f) + 2[S_1(f) * S_1(f)] \qquad (2.19)
\end{aligned}
$$

Similarly,

$$S_3(f) = 9[\int_{-\infty}^{\infty} S_1(f)\,df]^2\delta(f) + 6[S_1(f) * S_1(f) * S_1(f)] \qquad (2.20)$$

The first term in 2.19 is a d.c. signal and the second term gives the power spectral density of second order IMD, which is the convolution of the individual spectra. Similarly, in 2.20 first term represents the d.c. part while the third order IMD given by the second term is the convolved version of the individual spectra.

Chapter 3

Spread-Spectrum System with Different Modulation Schemes

In this chapter, an analysis of the asynchronous DS-CDMA communication system with BPSK and QPSK as modulation schemes is presented. Average signal-to-noise ratio at the output of the receiver is calculated.

3.1 CDMA With BPSK Modulation

The CDMA system model that we will consider is shown in Fig. 3.1 for K users [1]. The data stream $d_k(t)k = 1, \cdots, K$ of each user is modulated by a pseudo-noise sequence $c_k(t)$. The resulting wideband signal undergoes a second modulation using BPSK and transmitted. The transmitted signal for the kth user is given by

$$s_k(t) = \sqrt{2P}\, d_k(t)c_k(t)\cos(\omega_1 t + \phi_k) \tag{3.1}$$

The kth user's data signal $d_k(t)$ is a random sequence of unit amplitude, positive and negative rectangular pulses of duration T. $c_k(t)$ is the code sequence assigned to the kth user. ω_1 is the common carrier angular frequency, P is signal power and ϕ_k is the phase of the kth carrier.

The K transmitters in the system are assumed to be asynchronous. This is incorporated into the model by the introduction of a time delay for each transmitter so that the kth signal is delayed by an amount τ_k. τ_k is a time-delay parameter which accounts for propagation delay and the lack of synchronism between the signals. The received signal r(t) is given by

$$r(t) = n(t) + \sum_{k=1}^{K} s_k(t - \tau_k) \tag{3.2}$$

or

$$r(t) = n(t) + \sum_{k=1}^{K} \sqrt{2P}\, d_k(t - \tau_k)c_k(t - \tau_k)\cos(\omega_1 t + \theta_k) \tag{3.3}$$
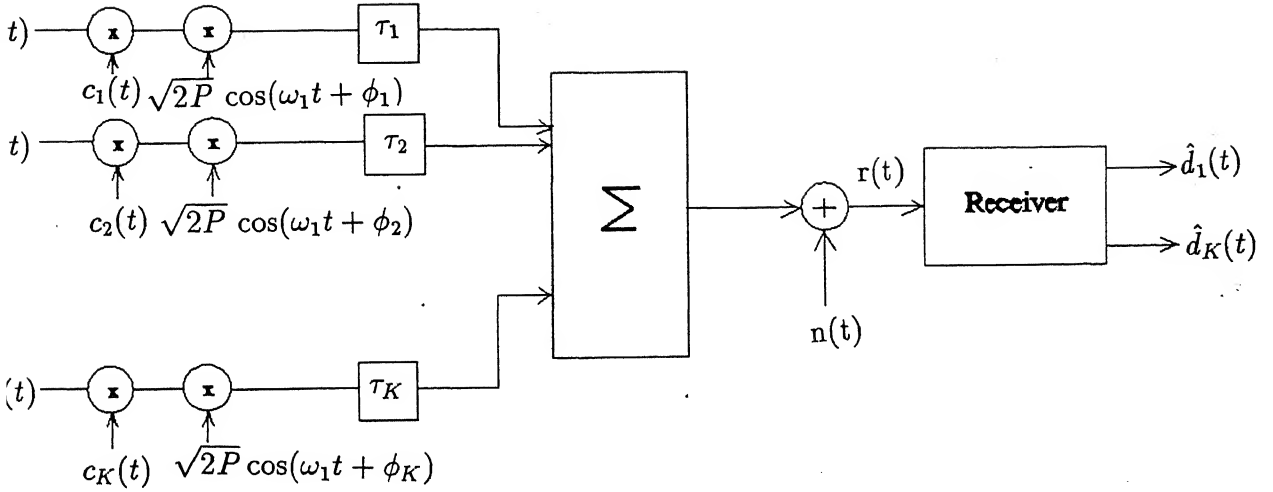
Figure 3.1: BPSK DS-SSMA system model

where $\theta_k = \phi_k - \omega_1 \tau_k$ and n(t) is the additive channel noise process which is assumed to be a white Gaussian process with two-sided power spectral density $\frac{N_0}{2}$. Since we are concerned with relative phase-shifts modulo 2π and relative time-delays modulo T, we may set $\tau_i = 0$ and $\theta_i = 0$ and consider only $0 \leq \tau_k < T$ and $0 \leq \theta_k < 2\pi$ for $k \neq i$. The parameters τ_k and θ_k are then the time delay and phase angle for the kth signal relative to the ith signal. The output of the correlation receiver [Fig. 3.2] matched to $s_i(t)$ is

$$Z_i = \int_0^T r(t) c_i(t) \cos \omega_1 t \, dt \tag{3.4}$$

The output of the correlation receiver at t=T is given by

$$Z_i = \sqrt{\frac{P}{2}} [d_{i,0} T + \sum_{k=1}^{K} \{ d_{k,-1} R_{k,i}(\tau_k) + d_{k,0} R'_{k,i}(\tau_k) \} \cos \theta_k] \tag{3.5}$$

$$+ \int_0^T n(t) c_i(t) \cos \omega_1 t \, dt \tag{3.6}$$

r(t) → ⊗ → ⊗ → $\int_0^T dt$ → $\hat{d}_i(t)$

$c_i(t)$ $\sqrt{2P}\cos\omega_1(t)$

Figure 3.2: BPSK Direct Sequence Spread Spectrum Receiver

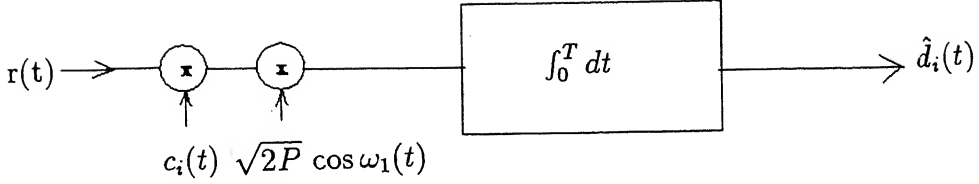where $d_{k,0}$ and $d_{k,-1}$ are the present and previous bits of the kth user during the interval [0,T], $d_{i,0}$ is the current bit during the interval [0,T] and $R_{k,i}$ and $R'_{k,i}$ are the continuous-time partial cross-correlation functions defined by

$$R_{k,i}(\tau_k) = \int_0^{\tau_k} c_k(t-\tau_k)c_i(t)\,dt \tag{3.7}$$

$$R'_{k,i}(\tau_k) = \int_{\tau_k}^T c_k(t-\tau_k)c_i(t)\,dt \tag{3.8}$$

for $0 \leq \tau_k \leq T$.
For $0 \leq lT_c \leq \tau_k \leq (l+1)T_c \leq T$, these two cross-correlation functions can be written as

$$R_{k,i}(\tau_k) = C_{k,i}(l-N)T_c + [C_{k,i}(l+1-N) - C_{k,i}(l-N)](\tau_k - lT_C) \tag{3.9}$$

and

$$R'_{k,i}(\tau_k) = C_{k,i}(l)T_c + [C_{k,i}(l+1) - C_{k,i}(l)](\tau_k - lT_c) \tag{3.10}$$

where the discrete aperiodic cross-correlation function $C_{k,i}$ for the sequences$(c_j^{(k)})$ and $(c_j^{(i)})$ is defined by

$$C_{k,i}(l) = \begin{cases} \sum_{j=0}^{N-1-l} c_j^{(k)} c_{j+l}^{(i)}, & 0 \leq l \leq N-1 \\ \sum_{j=0}^{N-1+l} c_{j-l}^{(k)} c_j^{(i)}, & 1-N \leq l < 0 \\ 0, & |l| \geq N. \end{cases}$$

where $c_j^{(k)}$ and $c_j^{(i)}$ are the jth bits of the kth and i^{th} users respectively.

To evaluate the signal-to-noise ratio at the output of the ith correlation receiver, the interference terms appearing in (2.14) are treated as additional noise. If $d_{i,0} = +1$, the desired signal component of Z_i is $\sqrt{\frac{P}{2}}T$. The variance of the noise component of Z_i is

$$
\begin{aligned}
Var\{Z_i\} &= \frac{P}{4T} \sum_{k=1_{k\neq i}}^{K} \int_0^T [R_{k,i}^2(\tau) + R_{k,i}'^2(\tau)]\, d\tau + \frac{1}{4}N_0 T \\
&= \frac{P}{4T} \sum_{k=1_{k\neq i}}^{K} \sum_{l=0}^{N-1} \int_{lT_c}^{(l+1)T_c} [R_{k,i}^2(\tau) + R_{k,i}'^2(\tau)]\, d\tau] + \frac{1}{4}N_0 T \quad (3.11)
\end{aligned}
$$

where the expectation has been computed with respect to the mutually independent random variables θ_k, τ_k, $d_{k,-1}$ and $d_{k,0}$ for $1 \leq k \leq K$ and $k \neq i$. It is assumed that θ_k is uniformly distributed on the interval $[0, 2\pi]$ and τ_k is uniformly distributed on the interval [0,T] for $k \neq i$. Also, the data symbols $d_{k,l}$ are assumed to take values $+1$ or -1 with equal probability for $k \neq i$.

Substituting for $R_{k,i}(\tau)$ and $R_{k,i}'(\tau)$ from 3.9 & 3.10 into 3.11 and upon evaluating the resulting integral we find that

$$
Var\{Z_i\} = \frac{PT^2}{12N^3}\left(\sum_{k=1_{k\neq i}}^{K} r_{k,i} \right) + \frac{1}{4}N_0 T \quad (3.12)
$$

where

$$
\begin{aligned}
r_{k,i} &= \sum_{l=0}^{N-1}[C_{k,i}^2(l-N) + C_{k,i}(l-N)C_{k,i}(l-N+1) \quad (3.13) \\
&\quad + C_{k,i}^2(l-N+1) + C_{k,i}^2(l) + C_{k,i}(l)C_{k,i}(l+1) + C_{k,i}^2(l+1)] \quad (3.14)
\end{aligned}
$$

or

$$
r_{k,i} = 2\mu_{k,i}(0) + \mu_{k,i}(1) \quad (3.15)
$$

where $\mu_{k,i}(n)$ are the cross-correlation parameters defined by

$$
\mu_{k,i}(n) = \sum_{l=1-N}^{N-1} C_{k,i}(l)C_{k,i}(l+N) \quad (3.16)
$$

The signal-to-noise ratio is $\frac{P}{2}T^2$ divided by the total noise, which is

$$
SNR_i = [(6N^3)^{-1} \sum_{k=1_{k\neq i}}^{K} r_{k,i} + \frac{N_0}{2E_b}]^{-1} \quad (3.17)
$$

where $E_b = PT$ is the bit energy.
Now since

$$(6N^3)^{-1} \sum_{k=1}^{K} r_{k,i} \approx \frac{(K-1)}{3N} \tag{3.18}$$

hence,

$$SNR_i \approx [\frac{K-1}{3N} + \frac{N_0}{2E_b}]^{-1} \tag{3.19}$$

The probability of error will be given by $Pe = Q\sqrt{SNR}$. Table 3.1 shows the probability of error achieved for different values of received power for different sequence lengths N and the number of users K.

Received Power in dBm	10 $\log_{10} Pe$								
	N=127			N=255			N=511		
	k=5	k = 10	k = 15	k=10	k = 15	k = 20	k=10	k = 20	k = 25
-100	$-9.1 \times 10^{+1}$	$-4.8 \times 10^{+1}$	$-3.4 \times 10^{+1}$	$-5.3 \times 10^{+1}$	$-4.1 \times 10^{+1}$	$-3.2 \times 10^{+1}$	$-6.5 \times 10^{+1}$	$-3.6 \times 10^{+1}$	$-3.0 \times 10^{+1}$
-90	$-1.9 \times 10^{+2}$	$-9.2 \times 10^{+1}$	$-6.2 \times 10^{+1}$	$-1.5 \times 10^{+2}$	$-1.0 \times 10^{+2}$	$-8.0 \times 10^{+1}$	$-2.4 \times 10^{+2}$	$-1.2 \times 10^{+2}$	$-1.0 \times 10^{+2}$
-80	$-2.1 \times 10^{+2}$	$-1.0 \times 10^{+2}$	$-6.9 \times 10^{+1}$	$-1.9 \times 10^{+2}$	$-1.2 \times 10^{+2}$	$9.7 \times 10^{+1}$	$-3.6 \times 10^{+2}$	$-1.7 \times 10^{+2}$	$-1.4 \times 10^{+2}$
-70	$-2.2 \times 10^{+2}$	$-1.0 \times 10^{+2}$	$-7.0 \times 10^{+1}$	$-1.9 \times 10^{+2}$	$-1.3 \times 10^{+2}$	$-9.9 \times 10^{+1}$	$-3.8 \times 10^{+2}$	$-1.3 \times 10^{+2}$	$-1.5 \times 10^{+2}$
-60	$-2.2 \times 10^{+2}$	$-1.0 \times 10^{+2}$	$-7.0 \times 10^{+1}$	$-1.9 \times 10^{+2}$	$-1.3 \times 10^{+2}$	$-9.9 \times 10^{+1}$	$-3.8 \times 10^{+2}$	$-1.3 \times 10^{+2}$	$-1.5 \times 10^{+2}$
-50	$-2.2 \times 10^{+2}$	$-1.0 \times 10^{+2}$	$-7.0 \times 10^{+1}$	$-1.9 \times 10^{+2}$	$-1.3 \times 10^{+2}$	$-9.9 \times 10^{+1}$	$-3.8 \times 10^{+2}$	$-1.3 \times 10^{+2}$	$-1.5 \times 10^{+2}$

Table 3.1

3.2 SSMA With QPSK Modulation

The asynchronous SSMA system model using QPSK as the modulation scheme is shown in Fig. 3.3 [2]. For each transmitter, there are two binary data signals $d_{2k-1}(t)$ and $d_{2k}(t)$ each of which is a sequence of unit amplitude, positive and negative, rectangular pulses of duration T. The kth transmitted signal is given by

$$\begin{aligned} s_k(t) &= \sum_{k=1}^{K} \sqrt{2P} d_{2k-1}(t) c_{2k-1}(t) \cos(\omega_1 t + \phi_k) \\ &\quad + \sum_{k=1}^{K} \sqrt{2P} d_{2k}(t) c_{2k}(t) \sin(\omega_1 t + \phi_k) \\ &= S_k^I(t) + S_k^Q(t) \end{aligned} \tag{3.20}$$

where $S_k^I(t)$ and $S_k^Q(t)$ are the in-phase and quadrature components of the kth transmitted signal respectively. The received signal r(t) is given by

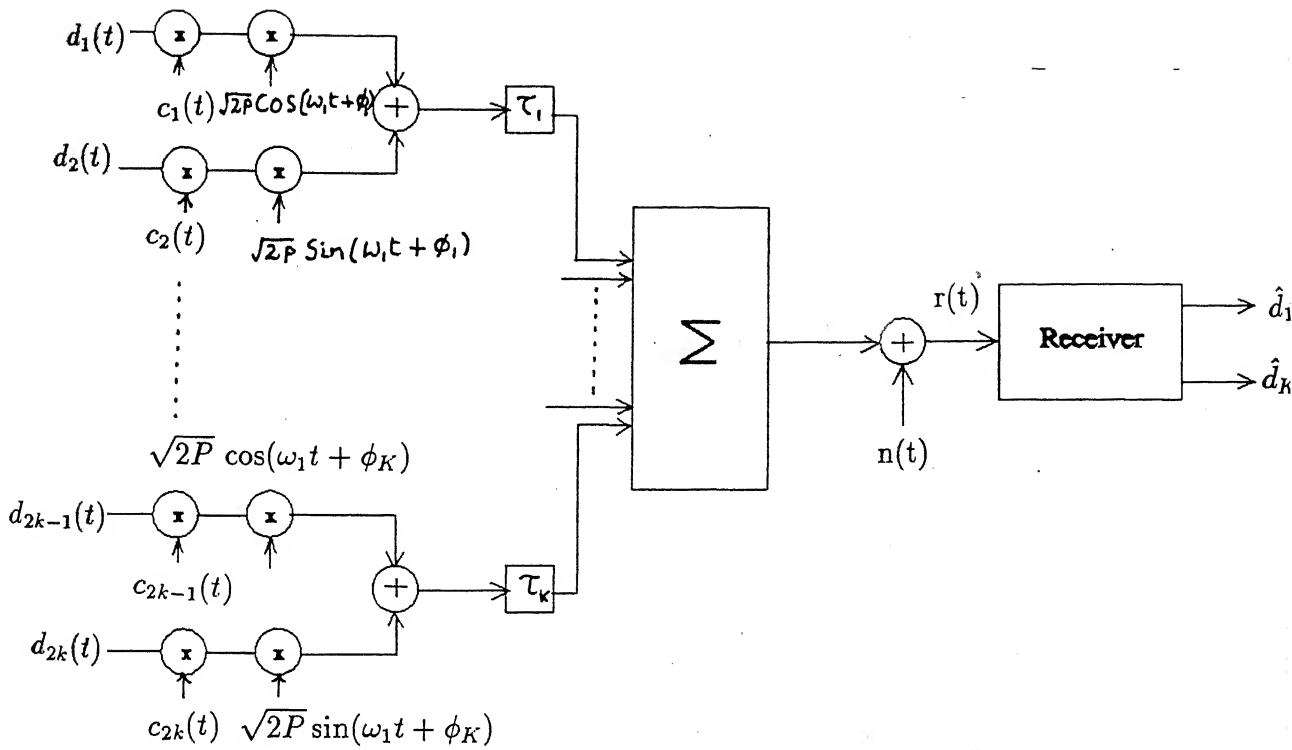$$r(t) = n(t) + \sum_{k=1}^{K} s_k(t - \tau_k)$$
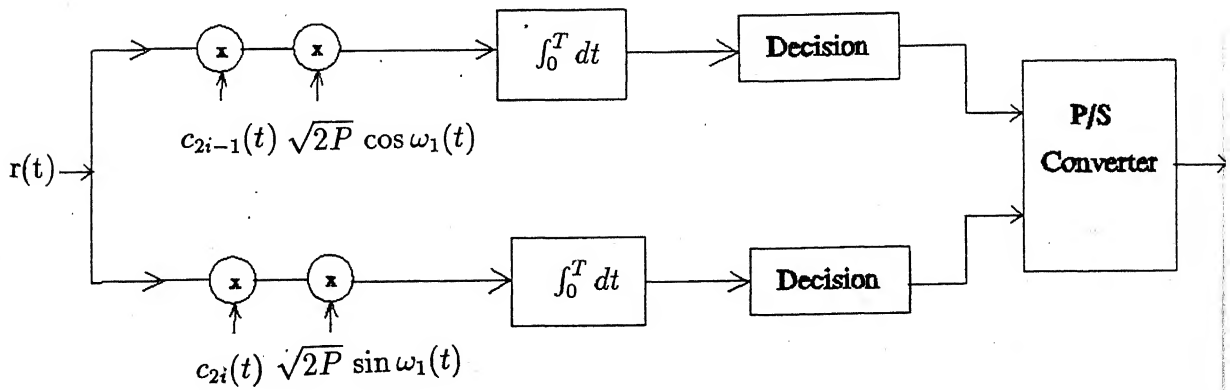
Figure 3.3: QPSK DS-SSMA communication system model

Figure 3.4: QPSK spread-spectrum receiver

$$= n(t) + \sum_{k=1}^{K} \sqrt{2P}\, d_{2k-1}(t - \tau_k) c_{2k-1}(t - \tau_k) \cos(\omega_1 t + \theta_k)$$

$$+ \sum_{k=1}^{K} \sqrt{2P}\, d_{2k}(t - \tau_k) c_{2k}(t - \tau_k) \sin(\omega_1 t + \theta_k)$$

$$= n(t) + S_k^I(t - \tau_k) + S_k^Q(t - \tau_k) \tag{3.21}$$

where $\theta_k = \phi_k - \omega_1 \tau_k$ and n(t) is the additive white Gaussian noise process with two-sided power spectral density $\frac{N_0}{2}$. Since relative time-delays and phase-shifts are important, we may set $\tau_i = 0$ and $\theta_i = 0$.

As shown in Fig. 3.4, the receiver for the kth signal consists of two parallel branches. Each branch is a correlation reciver which is matched to the appropriate signal component. The output of the in-phase correlation receiver for the ith signal is given by

$$
\begin{aligned}
Z_{2i-1} &= \int_0^T r(t) c_{2i-1}(t) \cos \omega_1 t \, dt \\
&= \int_0^T n(t) c_{2i-1}(t) \cos \omega_1 t \, dt \\
&\quad + \int_0^T \sum_{k=1}^{K} \sqrt{2P}\, d_{2k-1}(t - \tau_k) c_{2k-1}(t - \tau_k) c_{2i-1}(t) \\
&\quad \cos(\omega_1 t + \theta_k) \cos \omega_1 t \, dt \\
&\quad + \int_0^T \sum_{k=1}^{K} \sqrt{2P}\, d_{2k}(t - \tau_k) c_{2k}(t - \tau_k) c_{2i-1}(t) \\
&\quad \sin(\omega_1 t + \theta_k) \cos \omega_1 t \, dt
\end{aligned}
\tag{3.22}
$$

or

$$
\begin{aligned}
Z_{2i-1} &= \int_0^T n(t) c_{2i-1}(t) \cos \omega_1 t \, dt \\
&\quad + \int_0^T \sqrt{2P}\, d_{2i-1}(t) c_{2i-1}(t) \cos^2 \omega_1 t \, dt \\
&\quad + \int_0^T \sum_{k=1, k \neq i}^{K} \sqrt{\frac{P}{2}}\, d_{2k-1}(t - \tau_k) c_{2k-1}(t - \tau_k) c_{2i-1}(t) \\
&\quad [\cos(2\omega_1 t + \theta_k) + \cos \theta_k]\, dt \\
&\quad + \int_0^T \sqrt{2P}\, d_{2i}(t) c_{2i}(t) c_{2i-1}(t) \sin \omega_1 t \cos \omega_1 t \, dt \\
&\quad + \int_0^T \sum_{k=1, k \neq}^{K} \sqrt{\frac{P}{2}}\, d_{2k}(t - \tau_k) c_{2k}(t - \tau_k) c_{2i-1}(t) \\
&\quad [\sin(2\omega_1 t + \theta_k) + \sin \theta_k]\, dt
\end{aligned}
\tag{3.23}
$$

If the double-frequency terms are ignored, 3.23 may be written as

$$
\begin{aligned}
Z_{2i-1} =& \int_0^T n(t) c_{2i-1}(t) \cos \omega_1 t \, dt \\
&+ \sqrt{\frac{P}{2}} \, d_0^{(2i-1)} T \\
&+ \sqrt{\frac{P}{2}} \int_0^T \sum_{\substack{k=1 \\ k \neq i}}^{K} d_{2k-1}(t - \tau_k) c_{2k-1}(t - \tau_k) c_{2i-1}(t) \cos \theta_k \, dt \\
&+ \sqrt{\frac{P}{2}} \int_0^T \sum_{\substack{k=1 \\ k \neq i}}^{K} d_{2k}(t - \tau_k) c_{2k}(t - \tau_k) c_{2i-1}(t) \sin \theta_k \, dt
\end{aligned}
\tag{3.24}
$$

If $d_0^{(2i-1)} = 1$, 3.24 can be written as

$$
\begin{aligned}
Z_{2i-1} =& \int_0^T n(t) c_{2i-1}(t) \cos \omega_1 t \, dt \\
&+ \sqrt{\frac{P}{2}} T \\
&+ \sqrt{\frac{P}{2}} \sum_{\substack{k=1 \\ k \neq i}}^{K} [d_{-1}^{(2k-1)} R_{2k-1,2i-1}(\tau_k) + d_0^{(2k-1)} R'_{2k-1,2i-1}(\tau_k)] \cos \theta_k \\
&+ \sqrt{\frac{P}{2}} \sum_{\substack{k=1 \\ k \neq i}}^{K} [d_{-1}^{(2k)} R_{2k,2i-1}(\tau_k) + d_0^{(2k)} R'_{2k,2i-1}(\tau_k)] \sin \theta_k
\end{aligned}
\tag{3.25}
$$

where $R_{n,m}(\tau)$ and $R'_{n,m}(\tau)$ are the continuous time partial cross-correlation functions defined by 3.7 & 3.8. From 3.25, the desired signal component of Z_{2i-1} is $\sqrt{\frac{P}{2}} T$. Proceeding in the same manner as in [3.1], the variance of the noise component is given by

$$
\begin{aligned}
Var\{Z_{2i-1}\} =& \frac{P}{4T} \int_0^T \sum_{\substack{k=1 \\ k \neq i}}^{K} (|R_{2k-1,2i-1}(\tau)|^2 + |R'_{2k-1,2i-1}(\tau)|^2 \\
&+ |R_{2k,2i-1}(\tau)|^2 + |R'_{2k,2i-1}(\tau)|^2) \, d\tau + \frac{1}{4} N_0 T
\end{aligned}
\tag{3.26}
$$

$$
\begin{aligned}
Var\{Z_{2i-1}\} =& \frac{P}{4T} \sum_{\substack{k=1 \\ k \neq i}}^{K} \sum_{l=0}^{N-1} \int_{lT_c}^{(l+1)T_c} (|R_{2k-1,2i-1}(\tau)|^2 + |R'_{2k-1,2i-1}(\tau)|^2 \\
&+ |R_{2k,2i-1}(\tau)|^2 + |R'_{2k,2i-1}(\tau)|^2) \, d\tau + \frac{1}{4} N_0 T \\
=& \frac{P}{4T} \frac{T_c^3}{3} \sum_{\substack{k \\ k \neq i}} (r_{2k-1,2i-1} + r_{2k,2i-1}) + \frac{1}{4} N_0 T
\end{aligned}
\tag{3.27}
$$

where $r_{n,m}$ is defined by 3.15. The signal-to-noise ratio of the in-phase branch of the ith receiver is

$$SNR_{2i-1} = \frac{\frac{P}{2}T^2}{Var Z_{2i-1}}$$

$$= \sum_{k=1_{k\neq i}}^{K} \frac{1}{6N^3}(r_{2k-1,2i-1} + r_{2k,2i-1}) + \frac{N_0}{2E_b}]^{-1} \quad (3.28)$$

where $E_b = PT$ is the energy per data bit. A similar analysis applied to the output Z_{2i} of the quadrature branch of the ith receiver, we get

$$SNR_{2i} = [\sum_{k=1_{k\neq i}}^{K} \frac{1}{6N^3}(r_{2k,2i} + r_{2k-1,2i}) + \frac{N_0}{2E_b}]^{-1} \quad (3.29)$$

By comparing eq.(2.2.7) with the signal-to-noise ratio of the BPSK system analyzed in section 2.1, we see that QPSK system has the effect of doubling the number of interfering signals. Probability of error for in-phase branch is given by

$$p = Q(\sqrt{SNR_{2i-1}}) \quad (3.30)$$

Probability of error is given by

$$Pe = 2p - p^2 \quad (3.31)$$

Table 3.2 shows the variation of Pe with received power for N = 127 and different number of users K.

| Received Power in dBm | $10 \log_{10} Pe$ | | |
| | N=127 | | |
	k=5	k = 10	k = 15
-100	$-6.5 \times 10^{+1}$	$-3.3 \times 10^{+1}$	$-2.3 \times 10^{+1}$
-90	$-1.0 \times 10^{+2}$	$-5.0 \times 10^{+1}$	$-3.4 \times 10^{+1}$
-80	$-1.1 \times 10^{+2}$	$-5.3 \times 10^{+1}$	$-3.6 \times 10^{+1}$
-70	$-1.1 \times 10^{+2}$	$-5.3 \times 10^{+1}$	$-3.6 \times 10^{+1}$
-60	$-1.1 \times 10^{+2}$	$-5.3 \times 10^{+1}$	$-3.6 \times 10^{+1}$
-50	$-1.1 \times 10^{+2}$	$-5.3 \times 10^{+1}$	$-3.6 \times 10^{+1}$

TABLE 3.2

Chapter 4

Coherent CDMA/SCM/WDM Fiber Optic System

In this chapter CDMA/SCM/WDM system with BPSK and QPSK as modulation schemes has been analysed. Coherent (heterodyne) detection is used at the receiver. Signal-to-noise ratio and probability of error are calculated at the receiver output for different sequence lengths and number of sequences. The final results include the effects of multiple-access interference, intermodulation noise, shot noise and thermal noise. The emphasis is on the multiple-access interference and the intermodulation distortion which are found to be the main sources of degradation for the received signal performance.

4.1   The CDMA/SCM/WDM System Model

Fig. 4.1 shows the block diagram of the coherent CDMA/SCM/WDM system, where only a pair of transmitting and receiving stations are shown. Each destination node receives its signal from the corresponding receiver station. Each transmitting node generates data at a fixed rate of 2.048Mbps. The data stream $\{d_{ik}\}$, i=1,...,L and k=1,...,K of each user is multiplied by a pseudo-noise code sequence c_k, k=1,...,K. The code sequences assigned are receiver based. The resulting wideband signal modulates a subcarrier in BPSK or QPSK at frequency f_i, i=1,...,L. The transmitted signals at different frequencies are received by more than one antenna if necessary. The received signals at different frequencies are subcarrier multiplexed. The multiplexed signal phase modulates a laser emitting at a wavelenth λ_j, j=1,...,M. Optical signals from different laser sources having properly spaced peak emission wavelenths (λ_j) are wavelenth-division multiplexed (WDM) and are transmitted simultaneously over the same fiber. At the receiver a WDM device is used to demultiplex the signals at different wavelenths. The optical signal at one particular wavelength is coherent detected. For this, the received signal is linearly combined with a LO signal to downconvert it to some intermediate frequency. The original information is retained in the process. The resulting signal is then detected using a
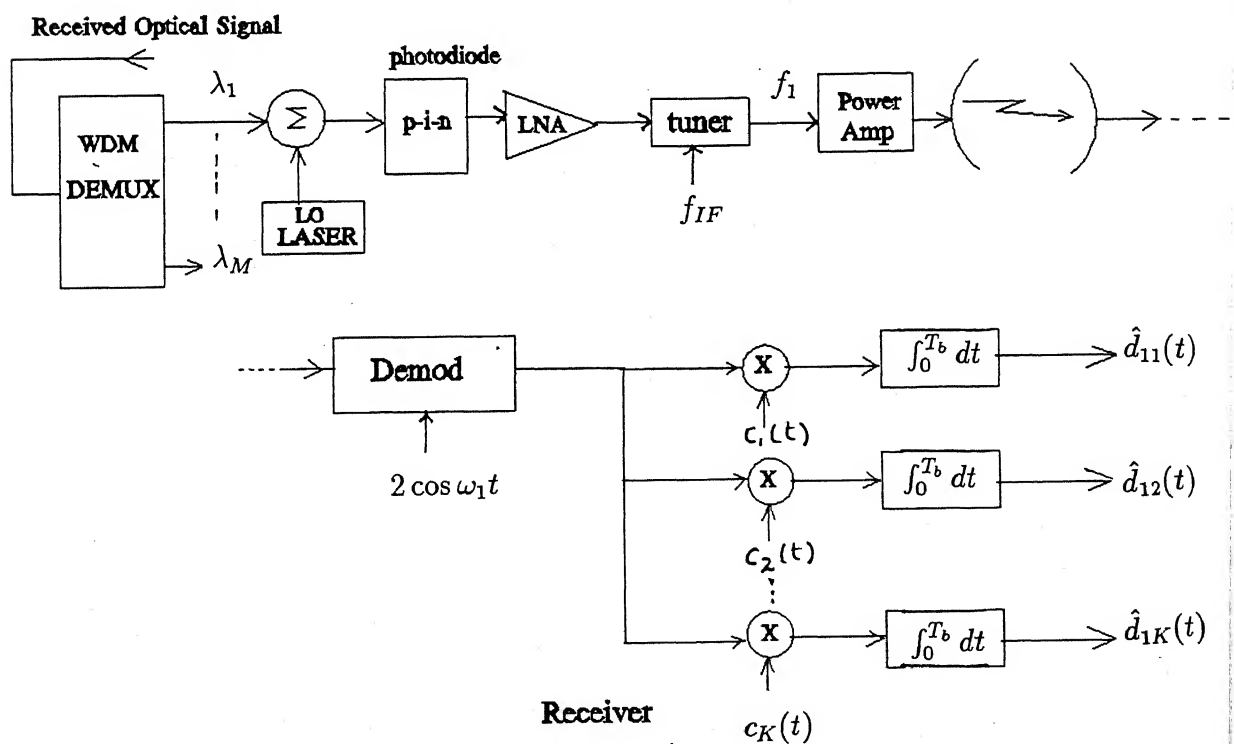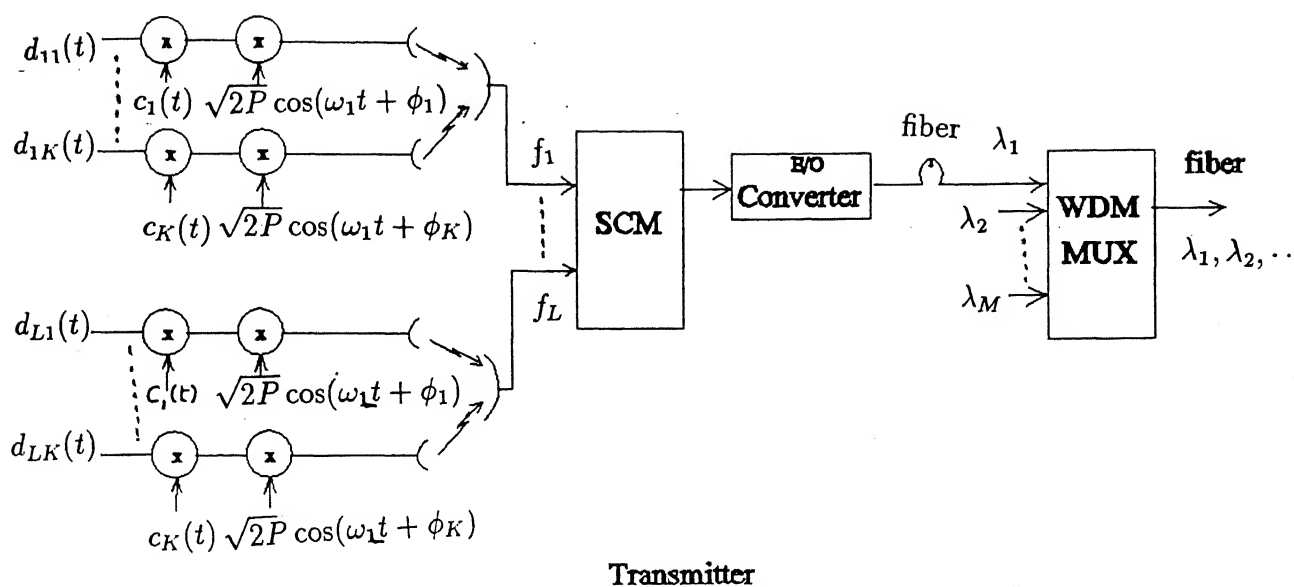
Figure 4.1: CDMA/SCM/WDM System Model

p-i-n photodiode. The bandpass filter (BPF) is tuned to f_i. The wavelength of the LO source, will be different for the different receiving stations. The output of the BPF, a modulated subcarrier, is transmitted to the different receivers. The received signal is demodulated and passed through a set of correlation receivers using different sequences c_k and the transmitted data is recovered.

Each receiving station is assigned a particular frequency and a fixed code sequence. Similarly, each transmitting station also has its own address identified by a particular frequency and a fixed code sequence. The set of code sequences used by the transmitting and receiving stations may be the same. However, to reduce interference, the transmitting and the receiving frequencies have to be different. If at the same time two different users try to call the same receiver, the call will be blocked and assumed to be lost.

4.2   System Analysis

The analysis is based on the following assumptions:

   1) Adjacent channel interference is negligible.
   2) Intersymbol interference is negligible.
   3) Users are at equal distances from the corresponding transmitting station.
   4) The different additive noises are assumed to be uncorrelated.
   5) Thermal noise is assumed to be white Gaussian with two-sided power spectral density $\frac{N_0}{2}$.
   6) The intermodulation noise, the shot noise and the multiple-access interference noise due to the interference of the stretching sequences are also assumed to be white Gaussian.

At the receiver, the detected photocurrent can be written as,

$$i(t) = R\{P_{LO} + P_s + 2\sqrt{P_{LO}P_s}\,\cos[2\pi f_{IF}t + \phi_m(t)]\} + n(t) \tag{4.1}$$

where

$$
\begin{aligned}
\phi_m(t) &= \sum_{i=1}^{L}\sum_{k=1}^{K} \beta_i c_k d_{ik} \cos[2\pi f_i t + \theta_k] \\
&= \sum_{i=1}^{L}\sum_{k=1}^{K} \beta_i \sin[\overline{2\pi f_i t + \theta_k + c_k d_{ik}\frac{\pi}{2}}] \quad .
\end{aligned}
\tag{4.2}
$$

with R the responsivity, P_{LO} the local oscillator power, P_s the received signal power of a subcarrier, f_{IF} the optical intermediate frequency, $\phi_m(t)$ the composite microwave signal, n(t) the additive noise process, L the number of subcarrier frequencies, K the number of users transmitting at the same frequency using CDMA, β_i the phase modulation index, and f_i the microwave subcarrier frequency.

The dc terms in (4.1) contain no information and can be ignored. Using Bessel's function expansion, (4.1) can be written as [8]

$$i(t) = 2R\sqrt{P_{LO}P_s}\sum_{k=1}^{K}\sum_{n_1=-\infty}^{\infty}\sum_{n_2=-\infty}^{\infty}\cdots\sum_{n_L=-\infty}^{\infty}J_{n_1}(\beta)J_{n_2}(\beta)\cdots J_{n_L}(\beta)$$

$$\cos\{2\pi[f_{IF}t + n_1(f_1t + \overline{\theta_k + c_k d_{ik}\frac{\pi}{2}}) + n_2(f_2t + \overline{\theta_k + c_k d_{ik}\frac{\pi}{2}})$$

$$+\cdots+ n_L(f_Lt + \overline{\theta_k + c_k d_{ik}\frac{\pi}{2}})]\} + n(t) \qquad (4.3)$$

where $J_n(\beta)$ denotes n^{th} order Bessel function of the first kind. The signal for the ith channel can be found by setting $n_i = -1$ and the remaining indices zero.

$$i_i(t) = 2R\sqrt{P_{LO}P_s}\sum_{k=1}^{K}J_1(\beta)[J_0(\beta)]^{L-1}\cos\{2\pi(f_{IF}-f_i)t - \overline{\theta_k + c_k d_{ik}\frac{\pi}{2}}\} \quad (4.4)$$

Since each subcarrier is a combination of K number of independent phase modulated carriers, the signal for the kth user of the ith channel is given by

$$i_{ik}(t) = 2R\sqrt{P_{LO}\frac{P_s}{K}}\,J_1(\beta)[J_0(\beta)]^{L-1}\cos\{2\pi(f_{IF}-f_i)t - \overline{\theta_k + c_k d_{ik}\frac{\pi}{2}}\} \qquad (4.5)$$

For obtaining the carrier-to-noise power ratio (CNR), the square of the rms current is used. With the photocurrent given by (4.4), the CNR of one of K components of the subcarrier becomes

$$CNR = \frac{2R^2\,P_{LO}\frac{P_s}{K}\,J_1^2(\beta)\,[J_0(\beta)]^{2N-2}}{\sigma_s^2 + \sigma_{th}^2 + \sigma_{sh}^2 + \sigma_{imd}^2} \qquad (4.6)$$

where σ_s^2, σ_{th}^2, σ_{sh}^2 and σ_{imd}^2 are the variances of multiple-access interference noise, thermal noise, shot noise and intermodulation noise, respectively, and the average power of each component is assumed to be the same. The thermal noise and the shot noise variances are given by

$$\sigma_{th}^2 = \frac{(N.F.)kTB}{R_L} \qquad (4.7)$$

$$\sigma_{sh}^2 = 2eRP_{LO}B \qquad (4.8)$$

where e is the electron charge, B the bandwidth of the bandpass filter, N.F. the amplifier noise figure, k the Boltzmann's constant, T the temperature in degrees Kelvin, and R_L the load resistance.

4.3 Intermodulation Distortion

The performance of multichannel SCM systems is degraded by the presence of the IMD. With coherent SCM systems, the IMD is a fundamental characteristic of the

nonlinear modulation format and the coherent detection process. When the transmission band is limited to a single octave, only third order IMD is of importance. For the 8-channel CDMA/SCM/WDM system operating in a multioctave configuration, both second- and third- order intermodulation products (IMPs) are significant contributors to the IMD. We first consider the effects of second-order IMD.

A second order IMD term is of the form $(f_i \pm f_j)$ and falls directly within the frequency band of the kth channel in an L-channel coherent SCM system when

$$|f_{IF} - (f_i \pm f_j)| = |f_{IF} - f_k| \qquad (4.9)$$

with the additional constraint $i \neq j$. By choosing the microwave subcarriers at odd frequencies, all second order terms occur at even frequencies and fall in between adjacent channels. This minimizes the degradation, but, does not eliminate it.

The magnitude of the intermodulation products is determined by the signal level and the phase-modulation index. From (4.13), the photocurrent for a single second-order IMP is

$$
\begin{aligned}
i_{2d}(t) = {} & 2R\sqrt{P_{LO}P_s} \sum_{k=1}^{K} J_1^2(\beta)[J_0(\beta)]^{L-2} \cos\{2\pi[f_{IF} - (f_i \pm f_j)]t \\
& - \overline{[\theta_{ik} + c_{ik}d_{ik}\frac{\pi}{2}} \pm \overline{\theta_{jk} + c_{jk}d_{jk}\frac{\pi}{2}]}\}
\end{aligned}
\qquad (4.10)
$$

It follows that the square of the rms current for the IMP is

$$< i_{2d} >_{rms}^2 = 2KR^2 P_{LO}P_s J_1^4(\beta)[J_0(\beta)]^{2L-4} \qquad (4.11)$$

and the total variance for the second order IMD is

$$\sigma_{2d}^2 = h_2 K_2 < i_{2d} >_{rms}^2 \qquad (4.12)$$

where K_2 is the number of second-order products and the factor h_2 takes into account the spectral form of the IMP and the associated filtering. The second-order IMP spectrum is a convolved version of the individual signal spectra and can be written as

$$S_{2IMP}(f) = S_i(f) * S_j(f) \qquad (4.13)$$

Where $S_i(f)$ and $S_j(f)$ are the spectra of the ith and the j_{th} carriers respectively. By definition, h_2 represents the fraction of the power that passes through the bandpass filter and is represented as

$$h_2 = \frac{\int_{-\infty}^{\infty} S_i(f) * S_j(f)|H(f)|^2 \, df}{\int_{-\infty}^{\infty} S_i(f) * S_j(f) \, df} \qquad (4.14)$$

Where H(f) is the frequency response of the band-pass filter.

The analysis for third-order intermodulation products is analogous to the approach described for the second-order intermodulation products. From the previous studies of third-order IMP's, it has been shown that products of the form $(f_h \pm f_i - f_j)$ are dominant in magnitude and number [12]. A third-order IMP that falls directly within the frequency band of the kth channel in an L-channel coherent SCM system satisfies the following condition

$$|f_{IF} - (f_h \pm f_i - f_j)| = |f_{IF} - f_k| \tag{4.15}$$

with the constraint $i \neq j \neq h$. Note that other intermodulation products such as $i = j \neq h$, are relatively small and not considered here [13].

The number of third order IMPs denoted as K_3 varies from channel to channel within a given system and is proportional to N^2. Furthermore, the centre channel has the most IMPs and the last channel has the least. The maximum number of third order products is bounded by $\frac{3N^2}{8}$. The photocurrent for the third order IMPs become

$$
\begin{aligned}
i_{3d}(t) &= 2R\sqrt{P_{LO}P_s} \sum_{k=1}^{K} J_1^3(\beta)[J_0(\beta)]^{L-3} \cos\{2\pi[f_{IF} - (f_h \pm f_i - f_j)]t \\
&\quad - \overline{[\theta_{hk} + c_{hk}d_{hk}\frac{\pi}{2}} \pm \overline{\theta_{ik} + c_{ik}d_{ik}\frac{\pi}{2}} - \overline{\theta_{jk} + c_{jk}d_{jk}\frac{\pi}{2}}]\}
\end{aligned}
\tag{4.16}
$$

The square of the rms current for the IMP is

$$< i_{3d} >_{rms}^2 = 2KR^2 P_{LO}P_s J_1^6(\beta)[J_0(\beta)]^{2L-6} \tag{4.17}$$

The variance of the third order IMD is given by

$$\sigma_{3d}^2 = h_3 K_3 < i_{3d} >_{rms}^2 \tag{4.18}$$

where K_3 is the number of third-order IMPs and h_3 is defined as

$$h_3 = \frac{\int_{-\infty}^{\infty} \{S_i(f) * S_j(f) * S_k(f)\}|H(f)|^2 \, df}{\int_{-\infty}^{\infty} S_i(f) * S_j(f) * S_k(f) \, df} \tag{4.19}$$

where $s_k(f)$ is the spectrum of the kth subcarrier. The spectrum for the third-order IMP is also a convolved version of the individual signal spectra, and can be written as

$$
\begin{aligned}
S_{3IMP}(f) &= S_i(f) * S_j(f) * S_k(f) \\
&= S_k(f) * S_{2IMP}(f)
\end{aligned}
\tag{4.20}
$$

Using 3.18, the signal-to-noise (SNR) for the coherent CDMA/SCM/WDM system including the second and third-order IMD and the shot noise can be written as

$$SNR = [\frac{K-1}{3N} + \frac{K\sigma_{th}^2}{2E_b} + \frac{K\sigma_{im}^2}{2E_b} + \frac{K\sigma_{sh}^2}{2E_b}]^{-1} \tag{4.21}$$

where

$$
\begin{aligned}
\sigma_{im}^2 &= 2h_2 K_2 R^2 P_{LO}P_s J_1^4(\beta)[J_0(\beta)]^{2L-4} \\
&\quad + 2h_3 K_3 R^2 P_{LO}P_s J_1^6(\beta)[J_0(\beta)]^{2L-6}
\end{aligned}
\tag{4.22}
$$

and

$$E_b = 2R^2 P_{LO}P_s J_1^2(\beta)[J_0(\beta)]^{2L-2} T_b \tag{4.23}$$
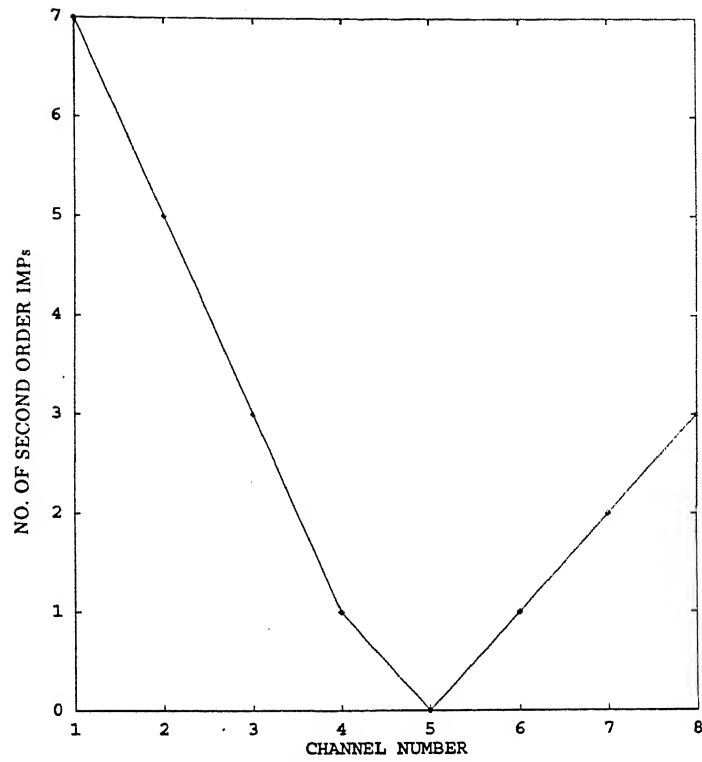
Figure 4.2: Number of Second order IMPs for an 8 Channel System
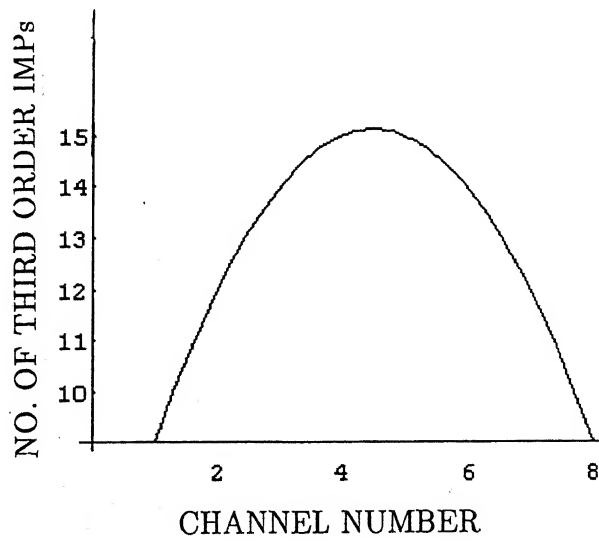
Figure 4.3: Number of Third order IMPs for an 8 Channel System

Approximating the Bessel functions to first order terms $[J_1(\beta) = \beta/2, J_0(\beta) = 1]$, the expression for the SNR reduces to

$$SNR = [\frac{K-1}{3N} + \frac{K\sigma_{th}^2}{2E_b} + \frac{K\sigma_{sh}^2}{2E_b}$$
$$+ \frac{[h_2 K_2 R^2 P_{LO} P_s(\frac{\beta^4}{8}) + h_3 K_3 R^2 P_{LO} P_s(\frac{\beta^6}{32})]}{2E_b}]^{-1} \qquad (4.24)$$

where $E_b = 0.5 R^2 P_{LO} P_s \beta^2 T_b$.

4.4 Results

Let us consider a CDMA/SCM/WDM system with 8 subcarrier multiplexed channels, each channel obtained by code-division multiple-access of K signals. Channel spacing depends upon the length of the PN sequence. For N=127 and input data rate of 2.048 Mbps, the channel spacing is 0.52 GHz and the subcarrier frequencies are $f_1 = 2.27$ GHz, $f_2 = 2.79$ GHz, ..., $f_8 = 5.91$ GHz. For this system, the calculated K_2 and K_3 are plotted in Fig. 4.2 and Fig. 4.3 respectively. Fig. 4.4 shows the spectra of two direct-sequence spread-spectrum signals at 3.31 GHz and 3.83 GHz and of their convolution which represents the spectrum of the second-order intermodulation product. Assuming the bandpass filter to be ideal and centered at 3.83 GHz and having a bandwidth of 0.52 GHz, the value of h_2 is found to be 0.5 from Fig. 4.4.

When all the channels have the same magnitude and spectral shape, h_2 becomes a constant for a given system. Similarly, with the help of Fig. 4.5 assuming an ideal bandpass filter centered at 3.83GHz and having a bandwidth of 0.52 GHz, h_3 turns out to be 0.92. Note that h_2 is smaller because the second-order distortion products occur between adjacent channels and are partially filtered out.

For the 8-channel CDMA/SCM/WDM system, Fig. 4.6 shows the plot of SNR as a function of the phase-modulation index β. The parameter values used are as follows:

R (the responsivity of photodetector) = 1A/w
P_{LO} (the local-oscillator power) = -2.6 dBm
P_s (received signal power) = -34 dBm
N.F. (amplifier noise-figure) = 3 dB
T (the temperature) = $300^0 K$
R_L (the load resistance) = 50Ω
K (Boltzmann's constant) = $1.38 \times 10^{-23} J/K$
B (the filter bandwidth) = 520 MHz
N (length of the PN sequence) = 127

From the plot it is clear that at low modulation indices, where the thermal and shot noise are dominant, the SNR increases with β. The curve then starts to level off and reaches a maximum. In this region, the IMD is of the same order of magnitude as the combined thermal and shot noise. Finally, increasing β further results in a SNR
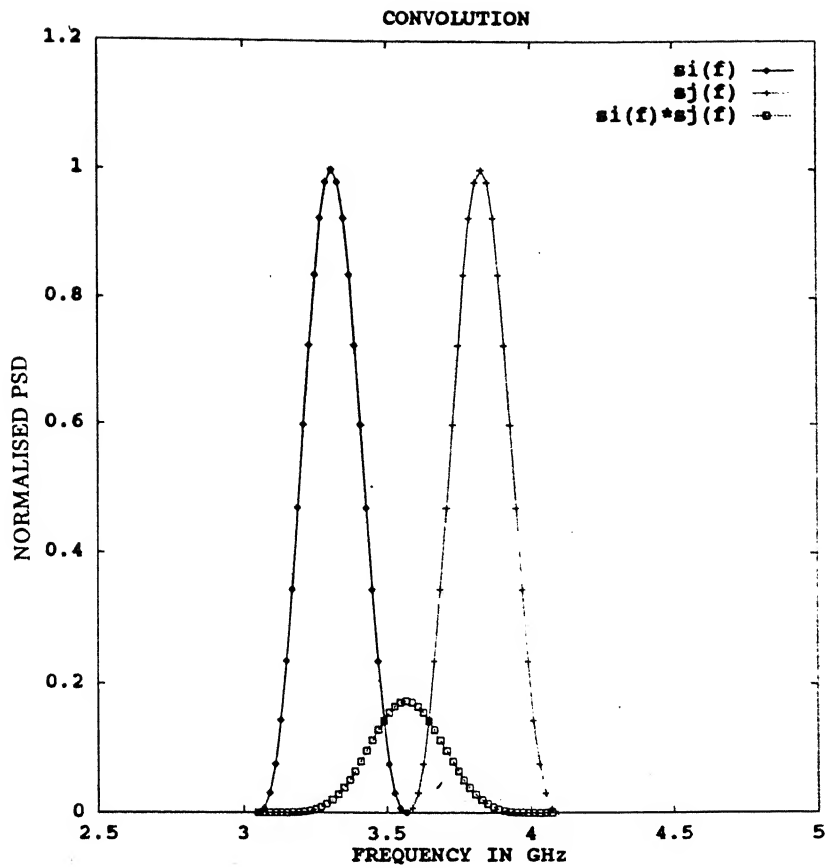
Figure 4.4: Bandpass Spectrum of a Single Second Order IMD Interfering Term (BPSK, N=127 and 2-6 GHz band)
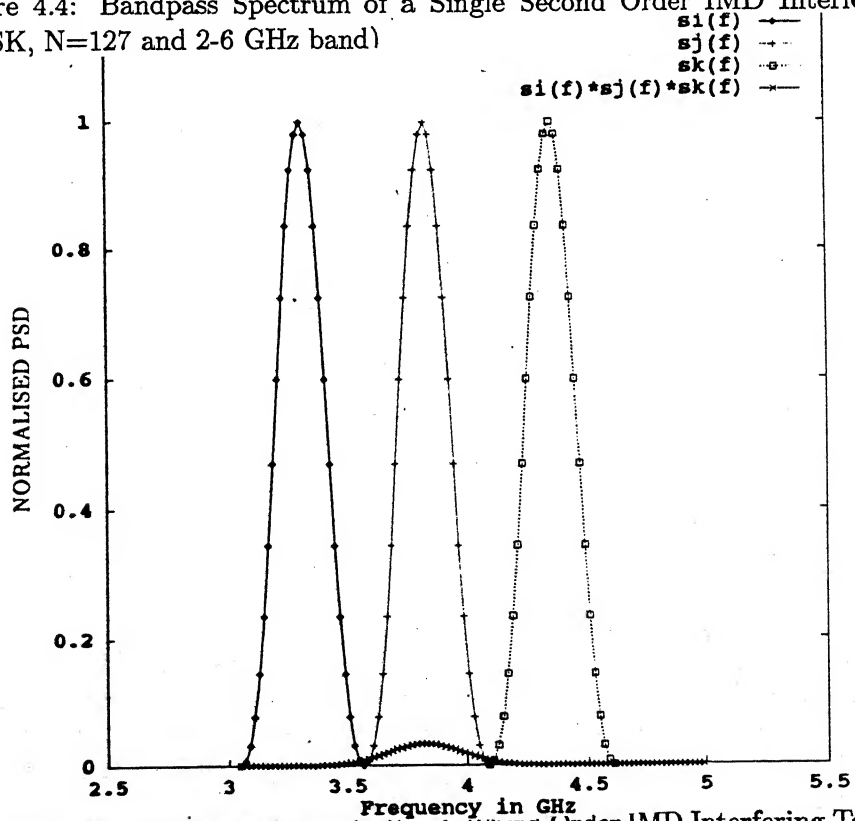
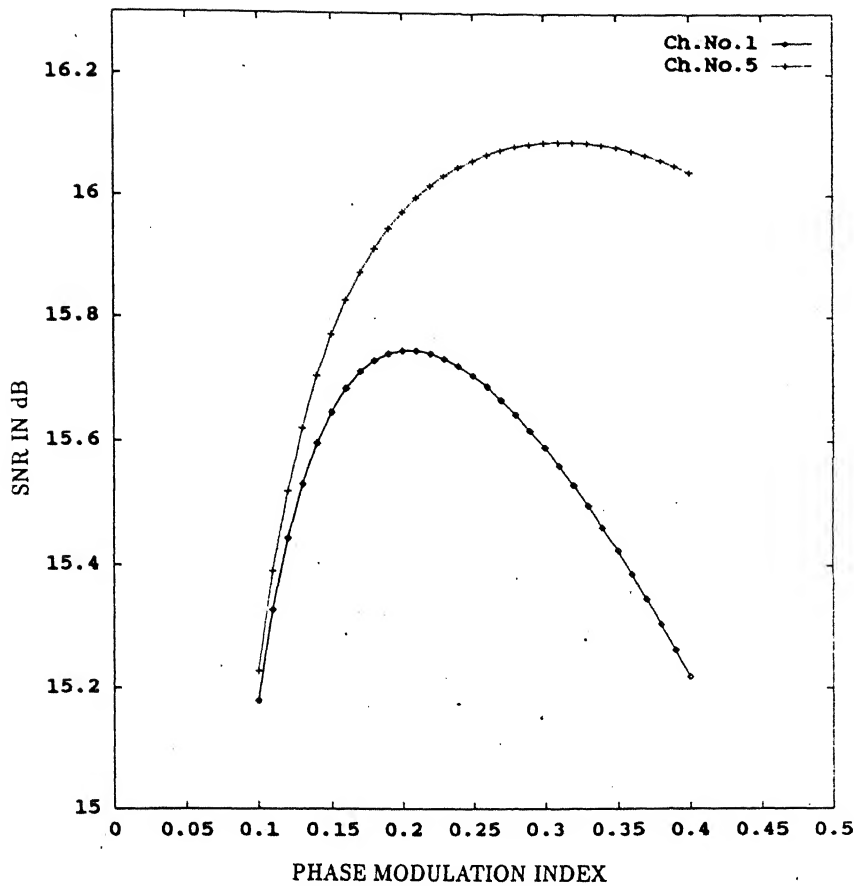Figure 4.5: Bandpass Spectrum of a Single Third Order IMD Interfering Term (BPSK, N=127 and 2-6 GHz band)

Figure 4.6: SNR vs. Phase Modulation Index for 8 Channel CDMA/SCM/WDM System (BPSK, N=127 and 2-6 GHz band)

degradation. Now the IMD is dominant, and the noise level increases faster than the signal. From the Fig. 4.6, optimal phase-modulation index is 0.2 for channel 1 and 0.31 for channel 5. Using these optimal values of β, the variation of probability of error with received power are shown in Fig. 4.7 - Fig. 4.9 for different values of K. Similar plots for N=255 and N=511 are shown in Fig. 4.14 - Fig. 4.21.

The variation of probility of error with the received power for QPSK and N=127 are shown in Fig. 4.22 - Fig. 4.24.

4.4.1 Discussion

For a fixed sequence length N and phase-modulation index β, probability of error increases with the number of users K for a given received power due to both decrease in signal power as well as increase in self noise.

The performance of the system improves as the sequence length N is increased. The system with large N can support more users than the system having small N with the same error probability. But the number of users is limited by the number of code sequences having good cross-correlation property.

There is an improvement in performance with increase in phase-modulation index β.

The performance of channel 5 is better than that of channel 1 since number of second-order products K_2 is zero for channel 5 and channel 1 has the most second-order IMPs.

The error floor present in the graphs implies that there is a minimum value of the probability of error that can be achieved in each case. Consider two different values of the received power P_s.

$P_s = -60$ dBm and N=127

        thermal noise $= 4 \times 10^{-29}$ watt/Hz
        shot noise $= 8 \times 10^{-29}$ watt/Hz
        intermodulation noise $= 8.1 \times 10^{-32}$ watt/Hz
        mutiple-access interference noise $= 6.9 \times 10^{-30}$ watt/Hz

and $P_s = -20$ dBm and N=127

        thermal noise $= 4 \times 10^{-29}$ watt/Hz
        shot noise $= 8 \times 10^{-29}$ watt/Hz
        intermodulation noise $= 8 \times 10^{-29}$ watt/Hz
        mutiple-access interference noise $= 6.9 \times 10^{-26}$ watt/Hz

As shown above, for low values of the received power, the thermal noise and the shot noise are dominant. As the received power increases, the signal dependent intermodulation noise power and multiple-access interference power increase and the SNR decreases. For very large values of the received power, the mutiple-access interference noise dominates and the error floor occurs.
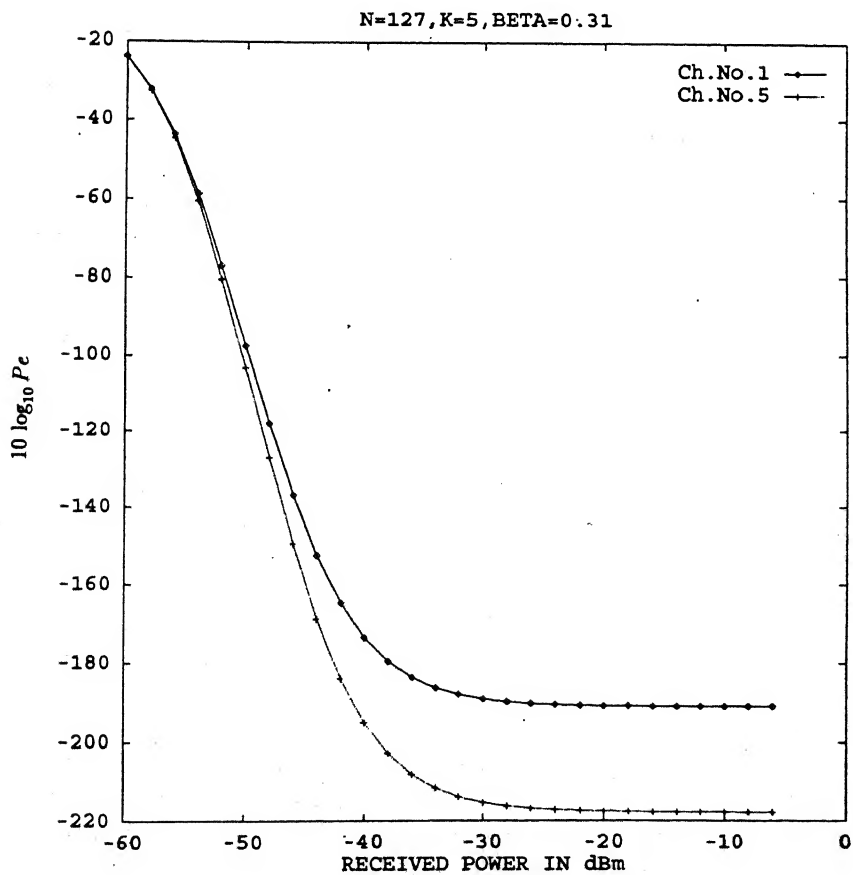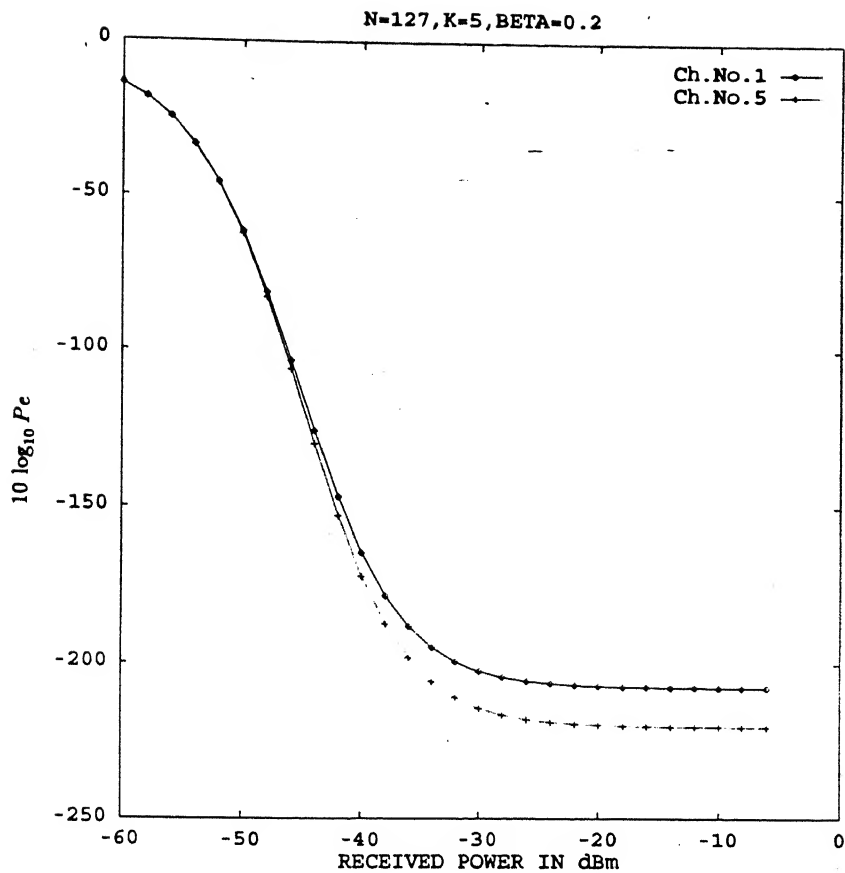
Figure 4.7: Probability of Error Vs. Received Power for N=127, k = 5 and 2-6 GHz band
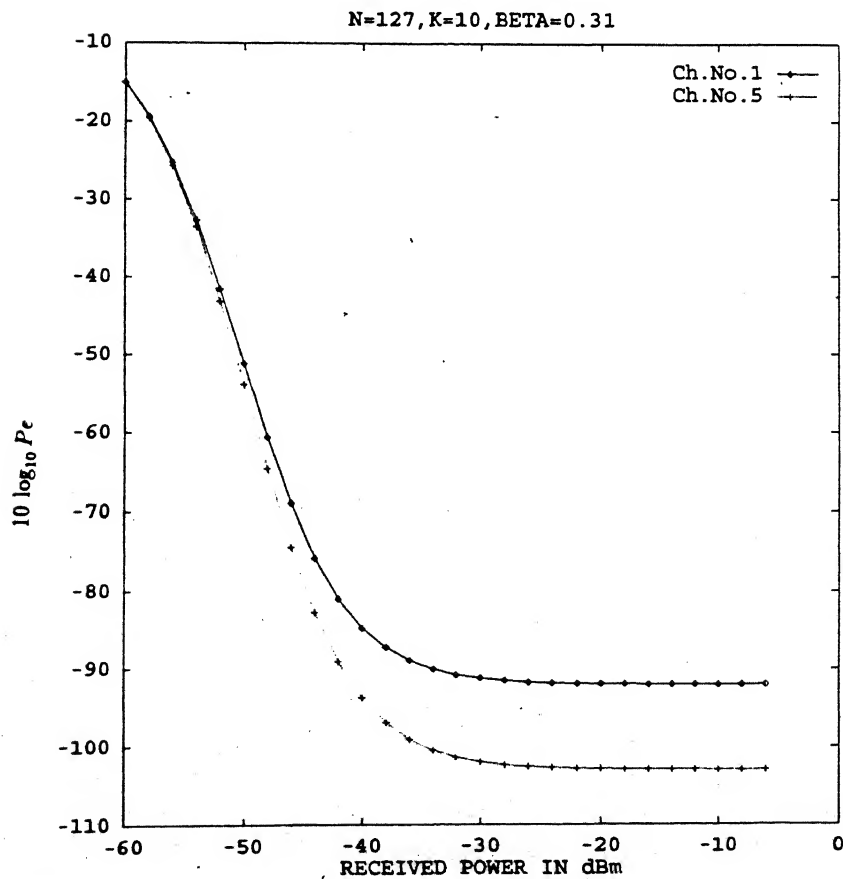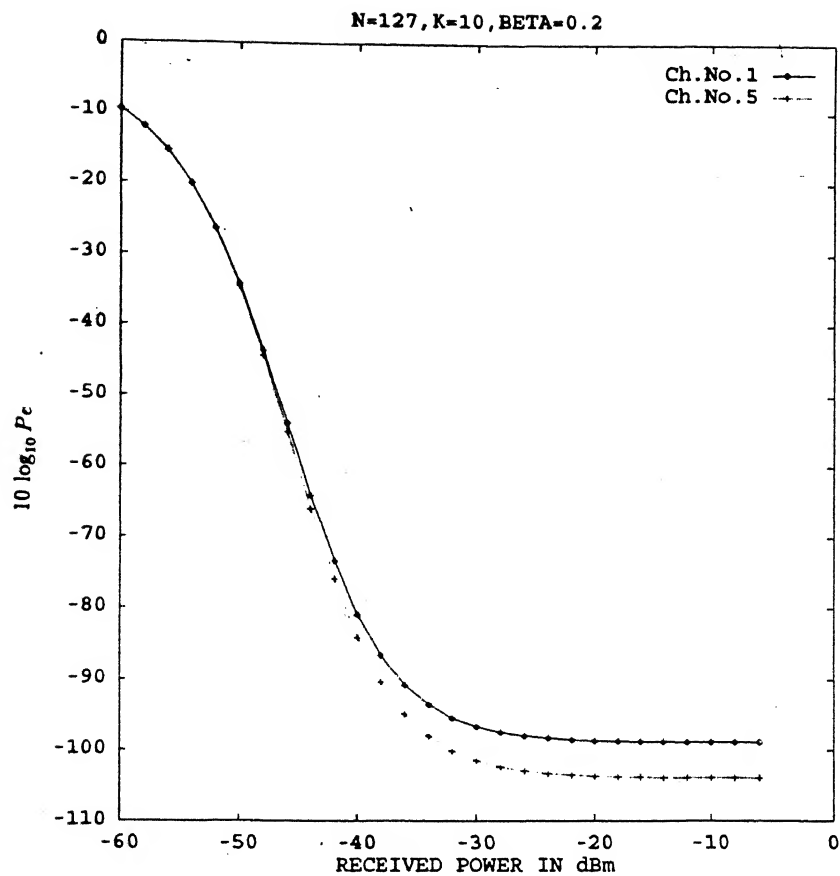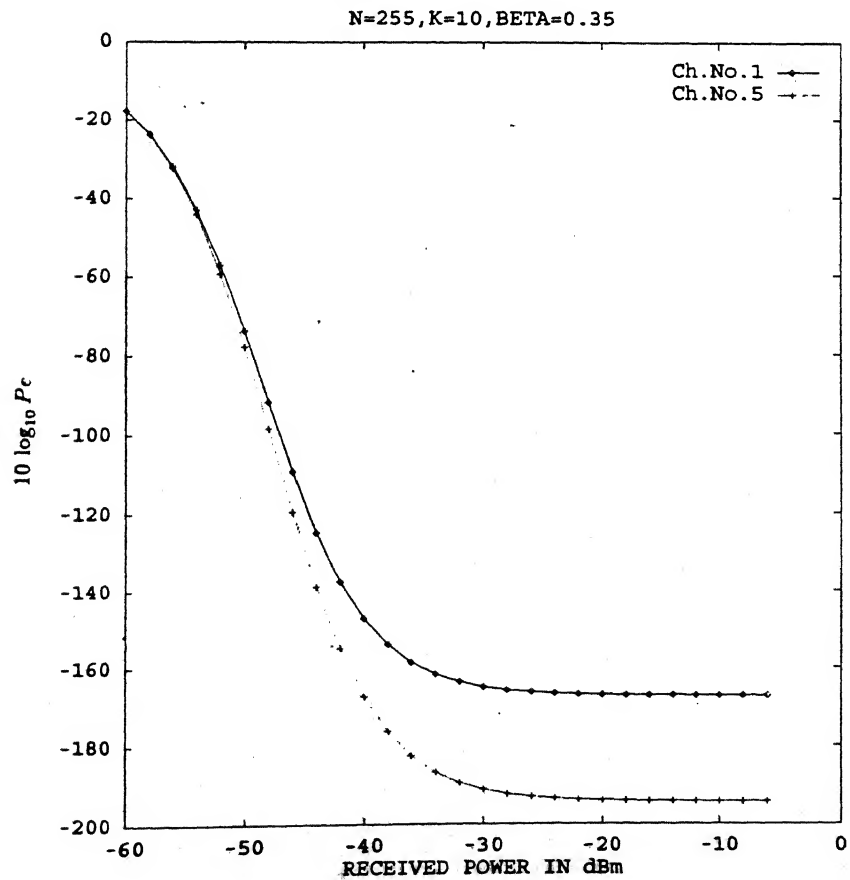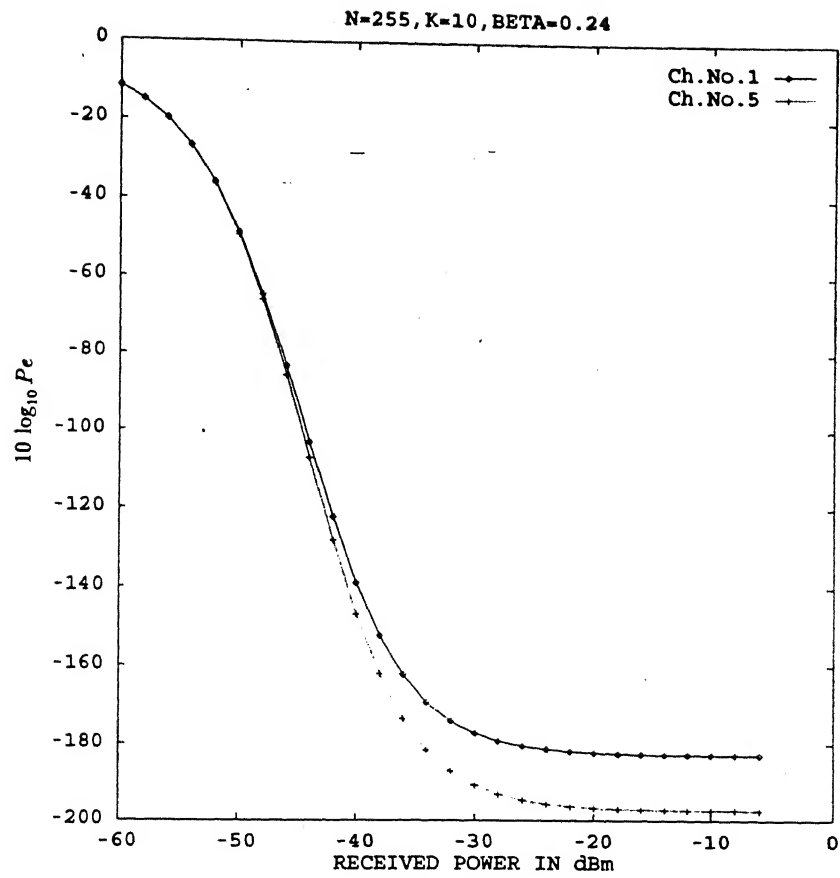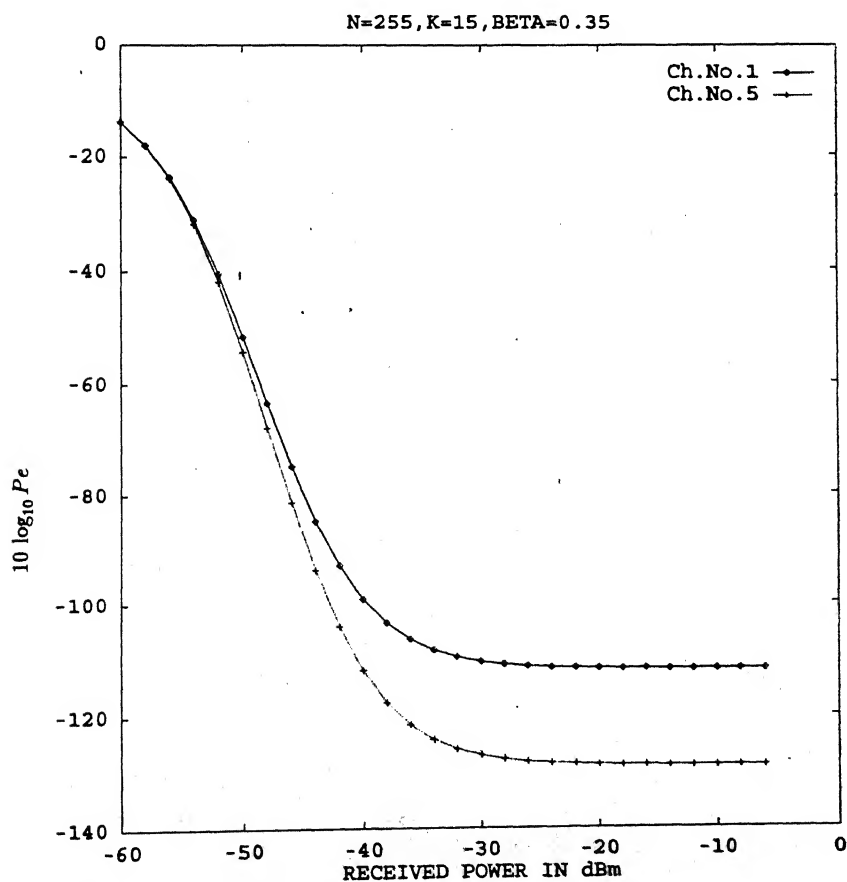
Figure 4.8: Probability of Error Vs. Received Power for N=127, k = 10 and 2-6 GHz band
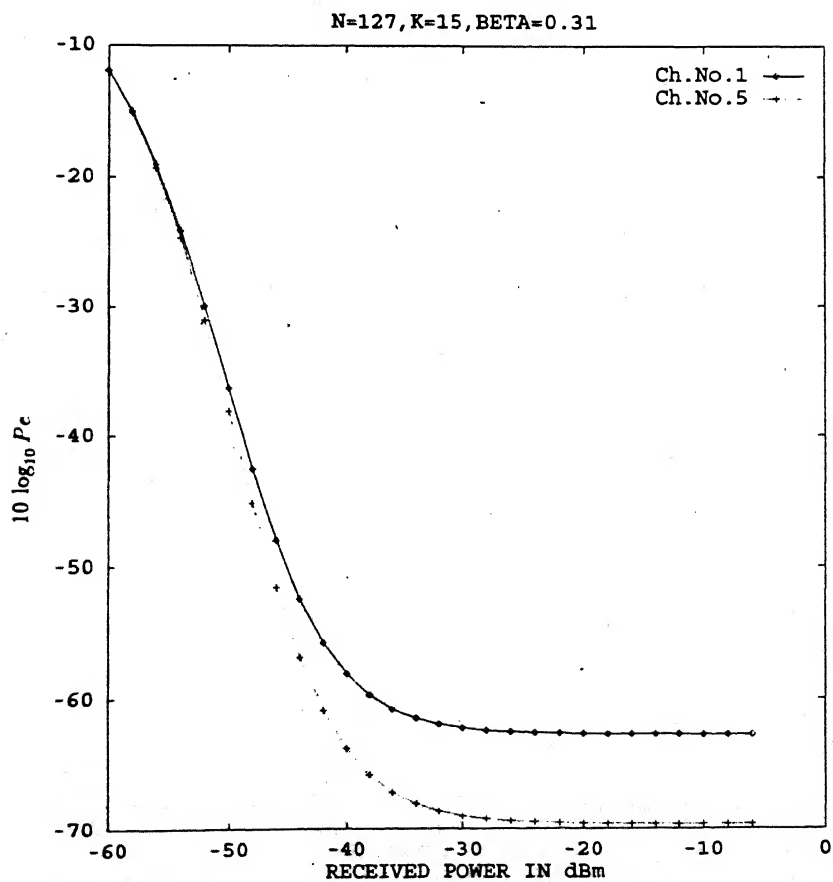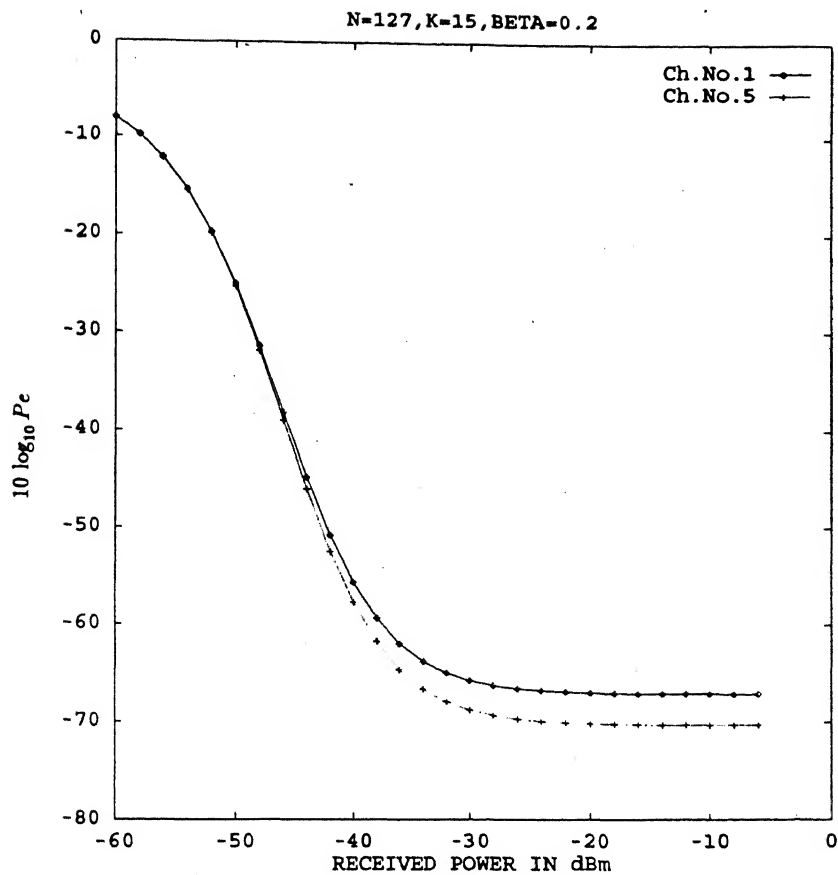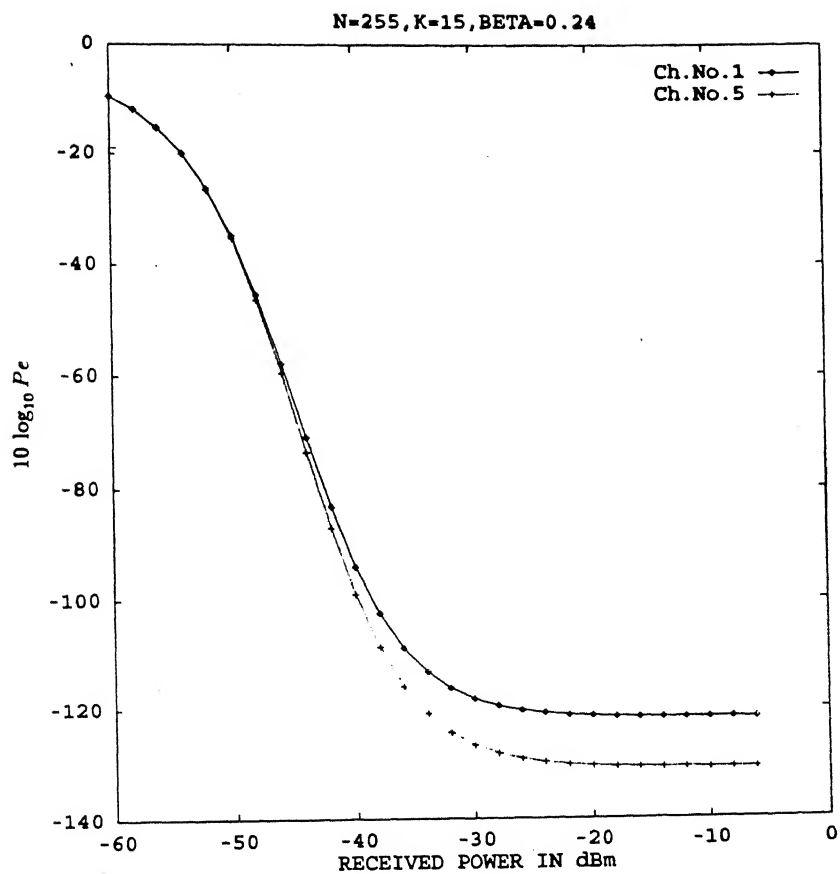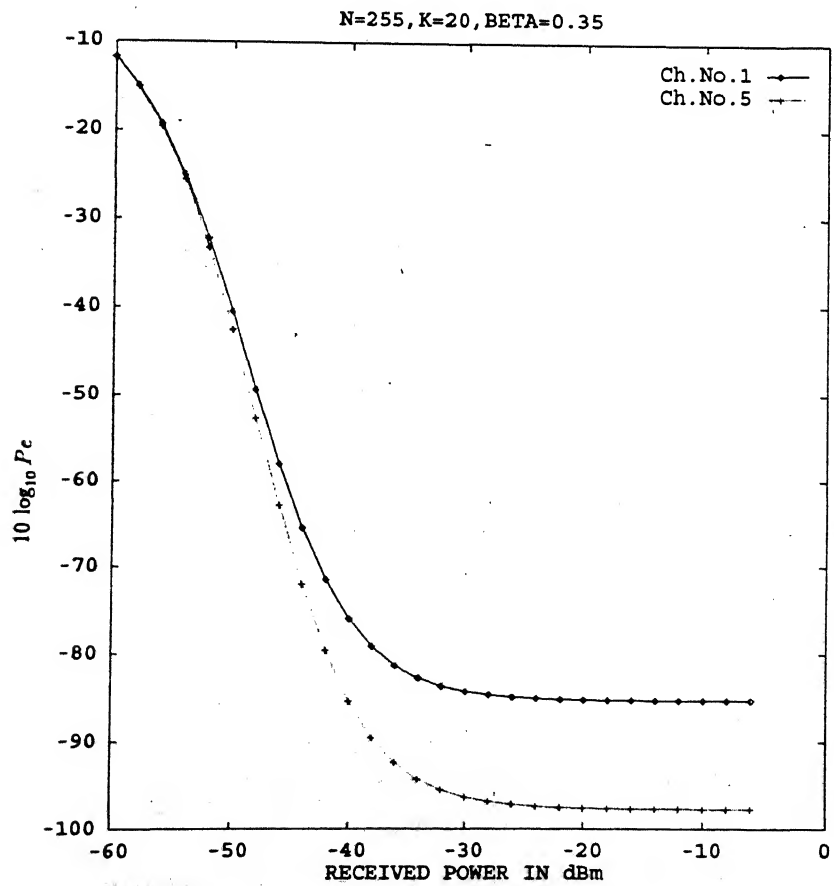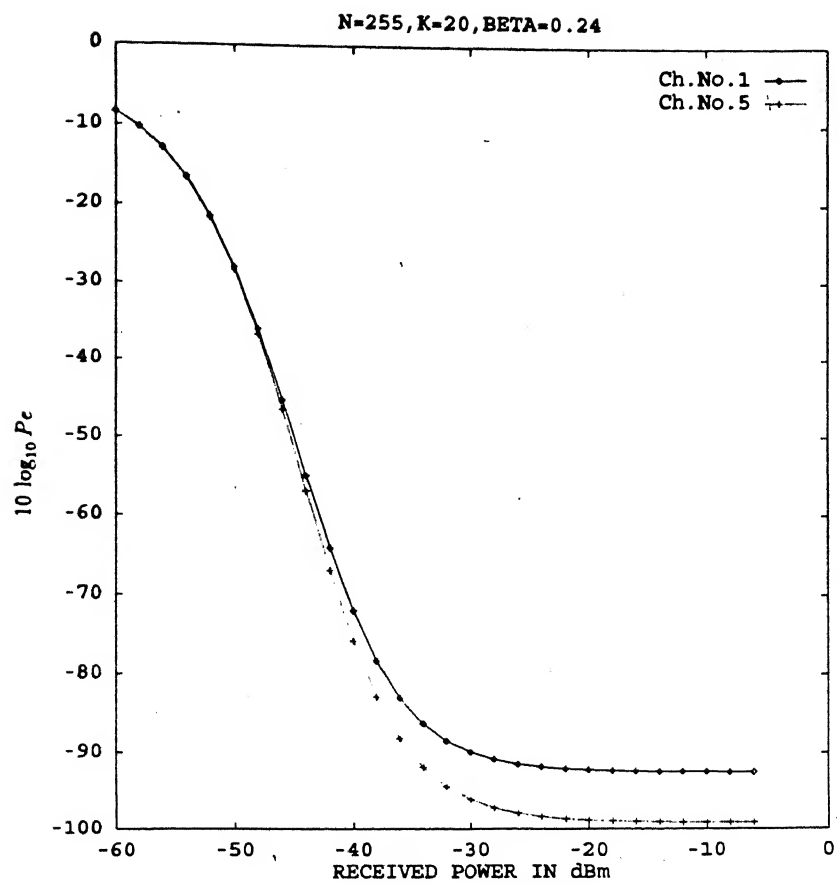
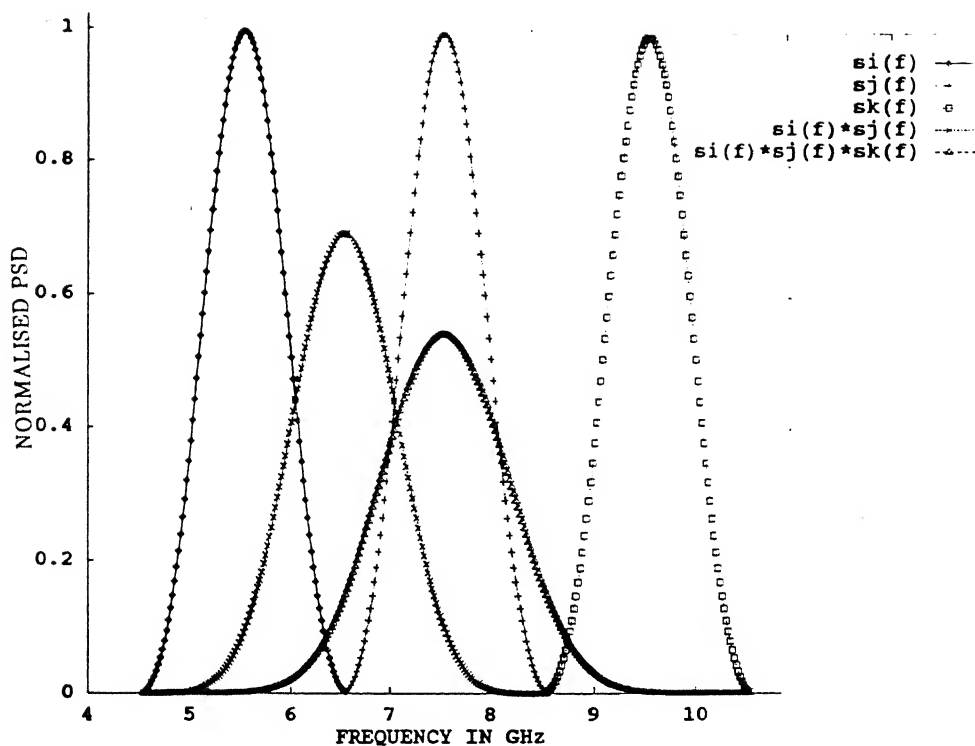Figure 4.9: Probability of Error Vs. Received Power for N=127, k = 15 and 2-6 GHz
band
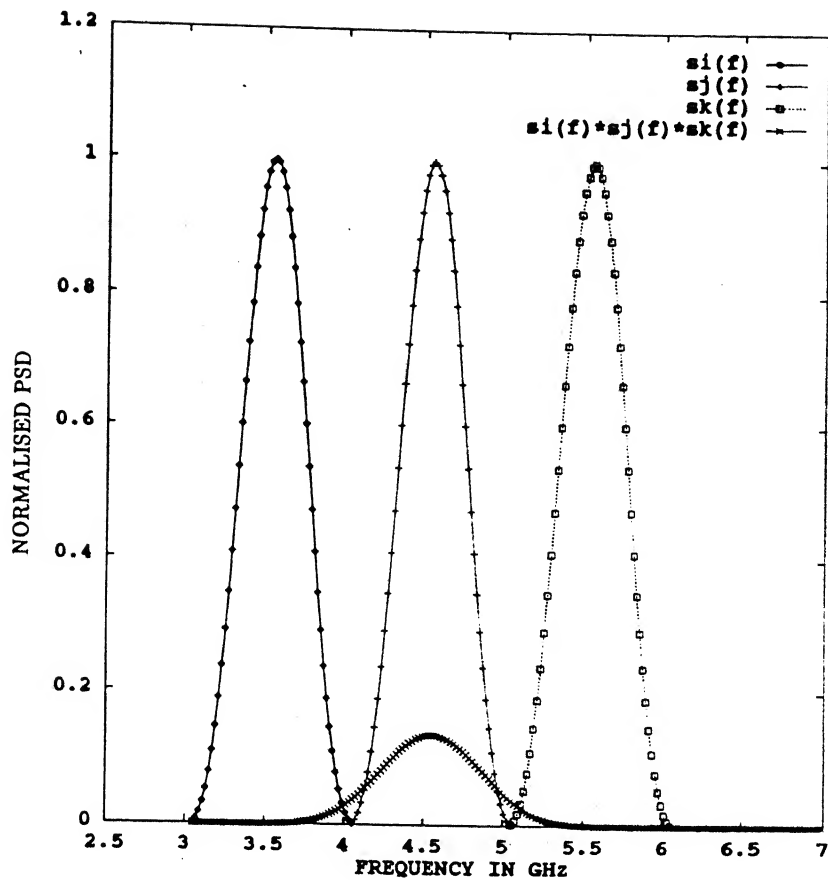
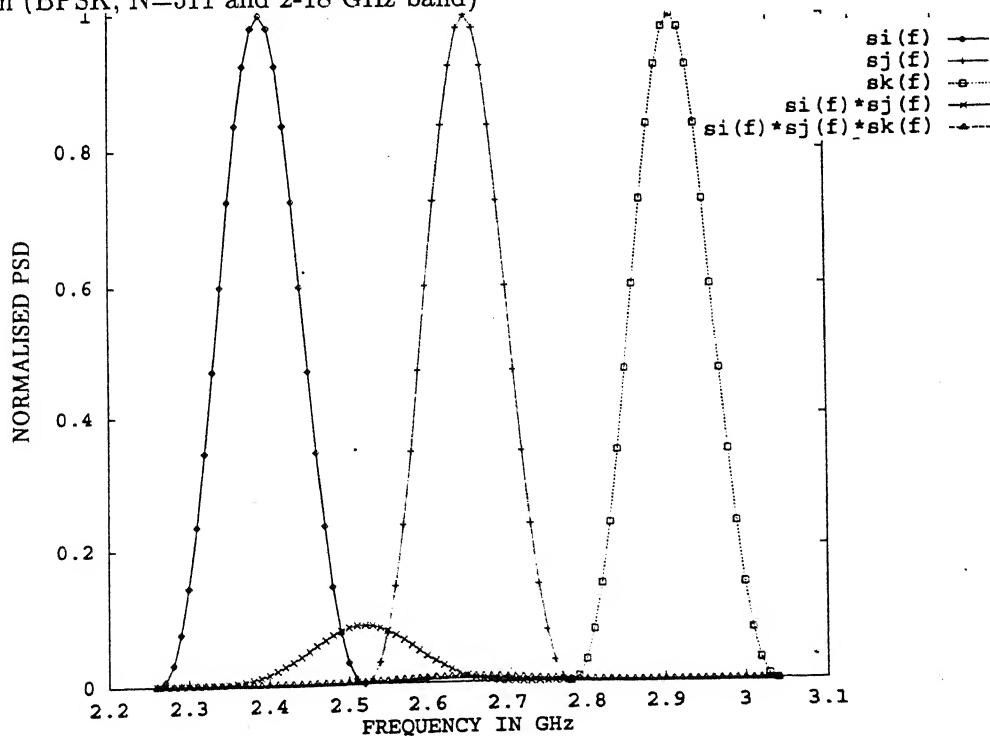Figure 4.10: Bandpass Spectrum of a Single Second Order IMD Interfering Term (BPSK, N=255 and 2-10 GHz band)
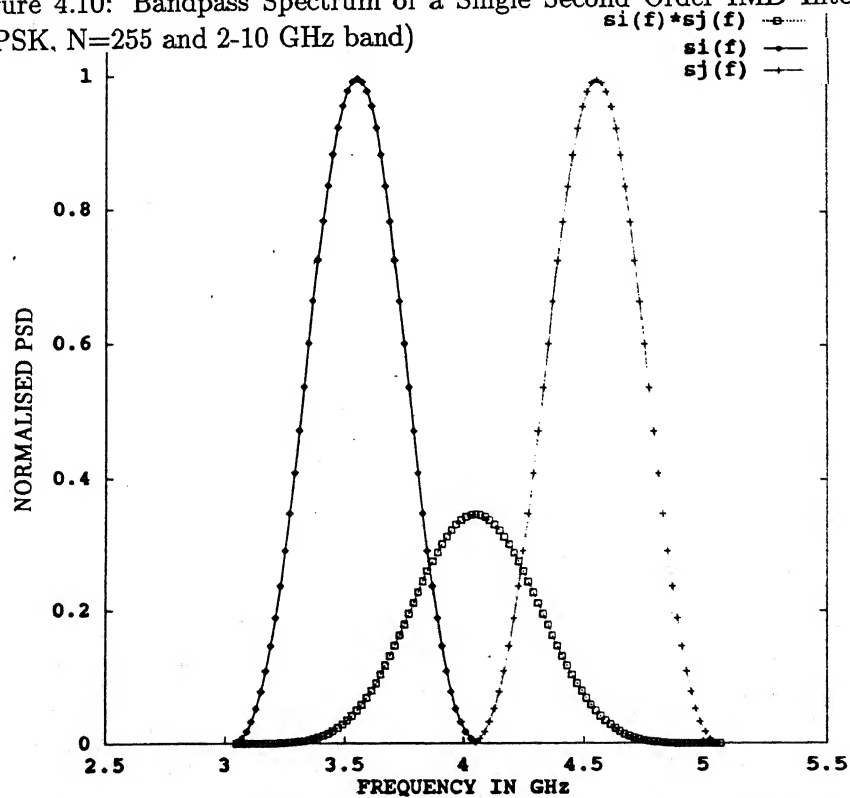
Figure 4.11: Bandpass Spectrum of a Single Third Order IMD Interfering Term (BPSK, N=255 and 2-10 GHz band)
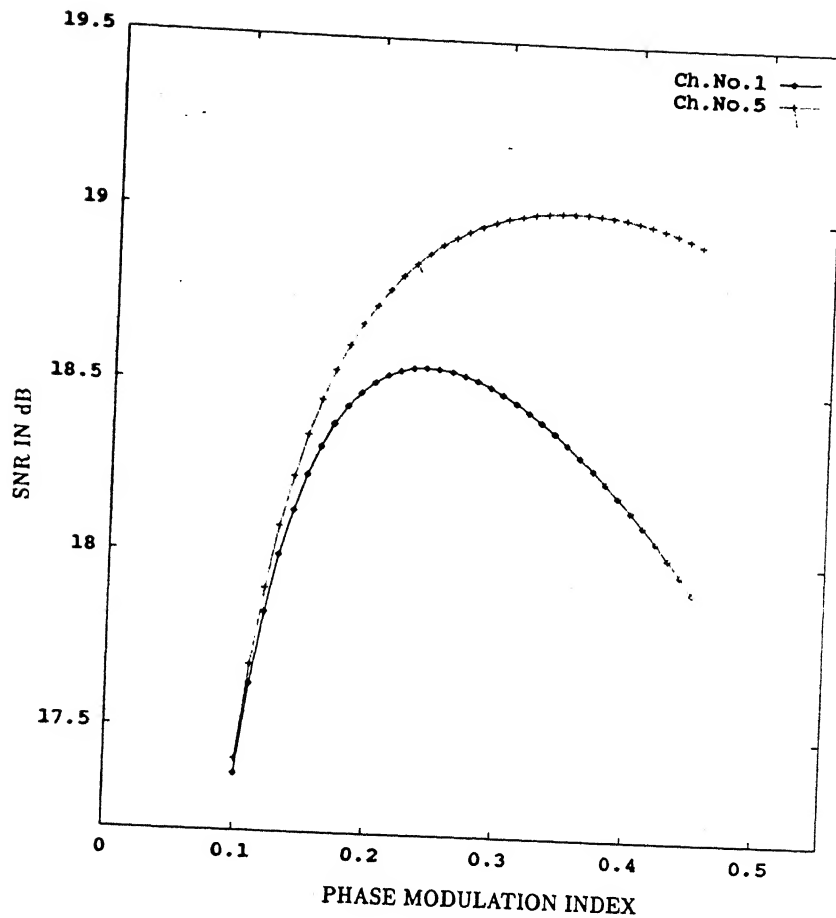
Figure 4.12: SNR vs. Phase Modulation Index for 8 Channel CDMA/SCM/WDM System (BPSK, N=255 and 2-10 GHz band)
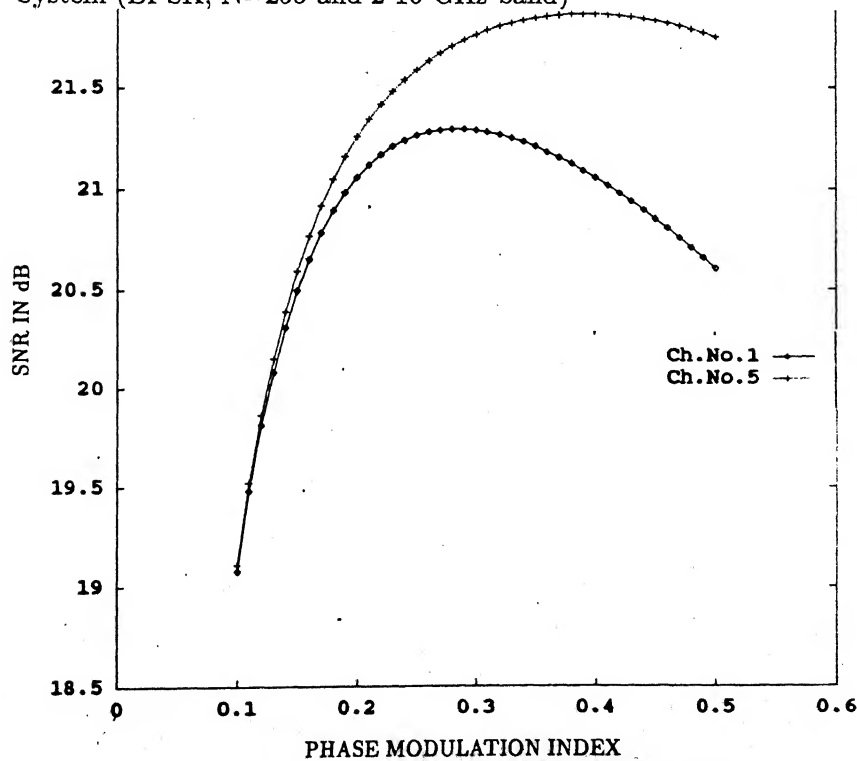
Figure 4.13: SNR vs. Phase Modulation Index for 8 Channel CDMA/SCM/WDM System (BPSK, N=511 and 2-18 GHz band)

N=255,K=10,BETA=0.24

N=255,K=10,BETA=0.35

Figure 4.14: Probability of Error Vs. Received Power for N=255, k = 10 and 2-10

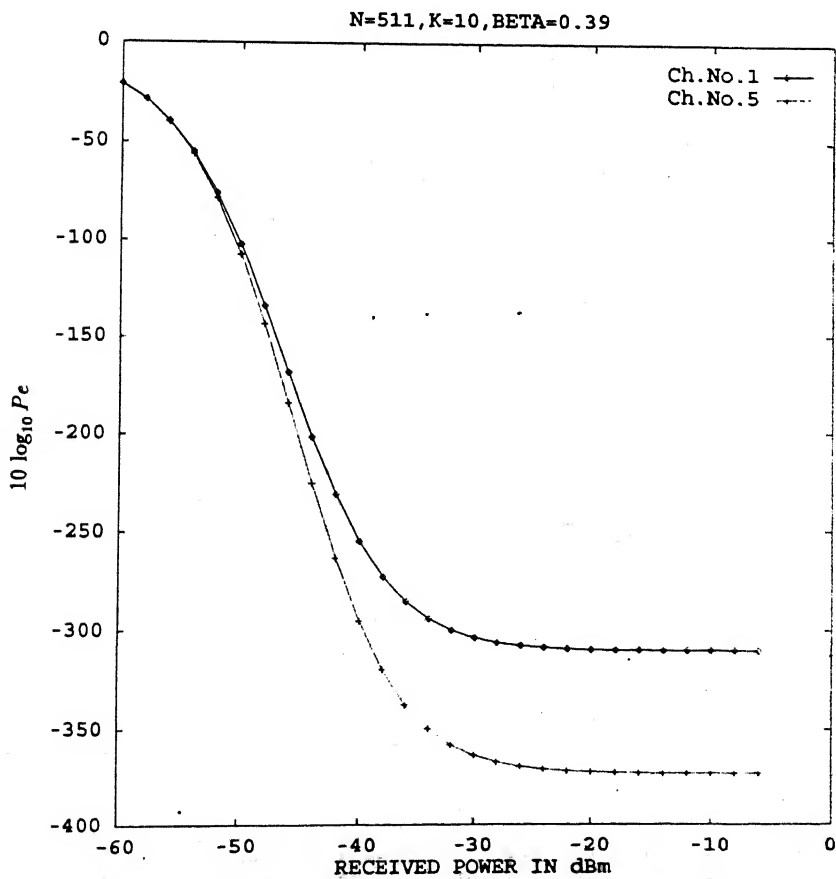Figure 4.15: Probability of Error Vs. Received Power for N=255, k = 15 and 2-10

Figure 4.16: Probability of Error Vs. Received Power for N=255, k = 20 and 2-10 GHz band

Figure 4.17: Bandpass Spectrum of a Single Second and Third Order IMD Interfering Term (BPSK, N=511 and 2-18 GHz band)

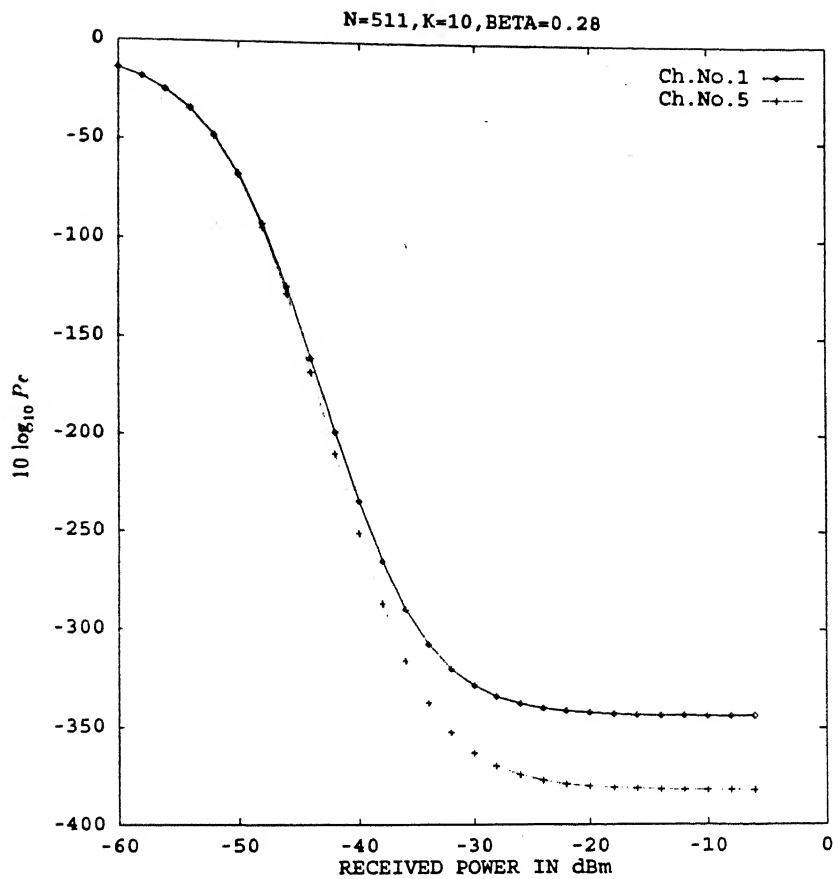Figure 4.18: Bandpass Spectrum of a Single Second Order IMD Interfering Term (QPSK, N=127 and 2-4 GHz band)

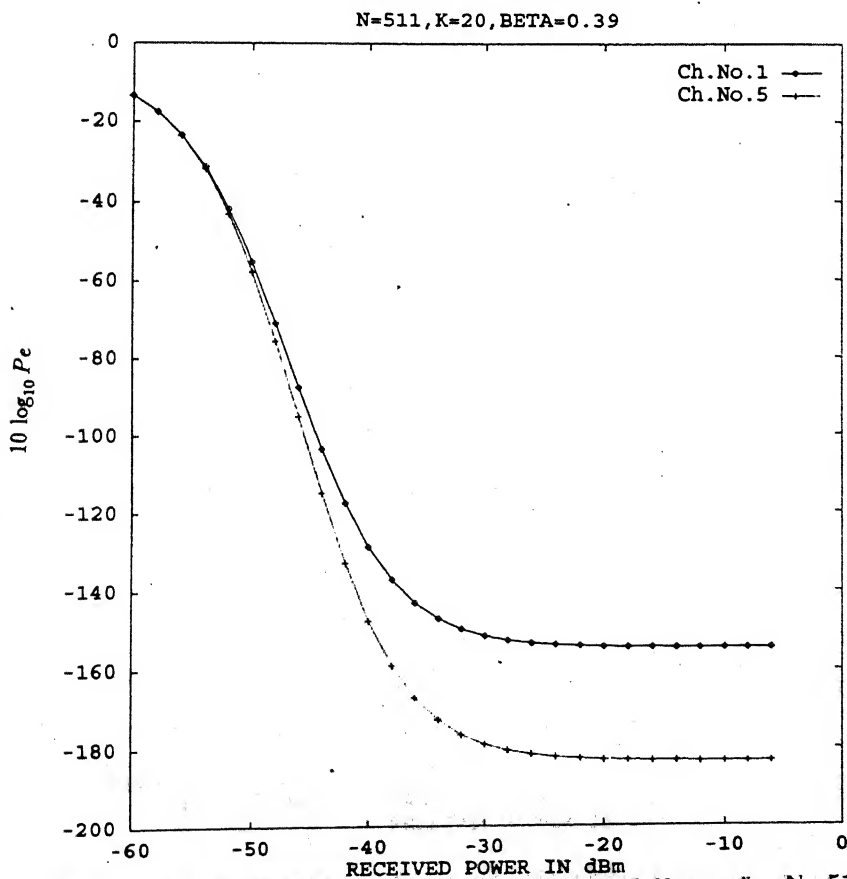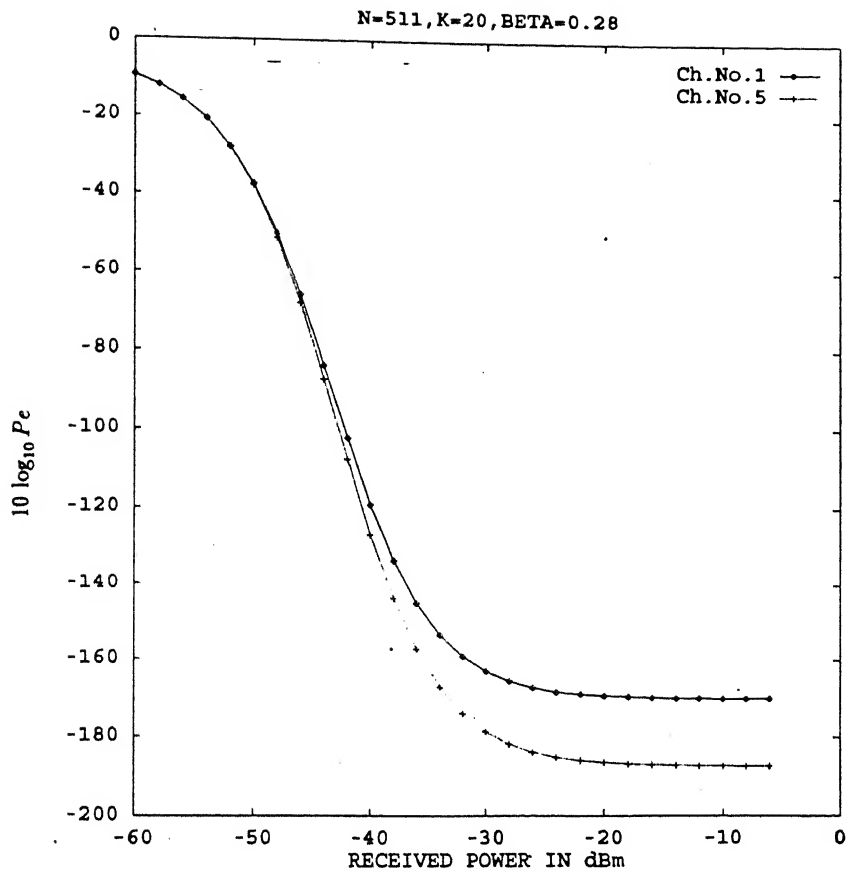Figure 4.19: Probability of Error Vs. Received Power for N=511, k = 10 and 2-18 GHz band

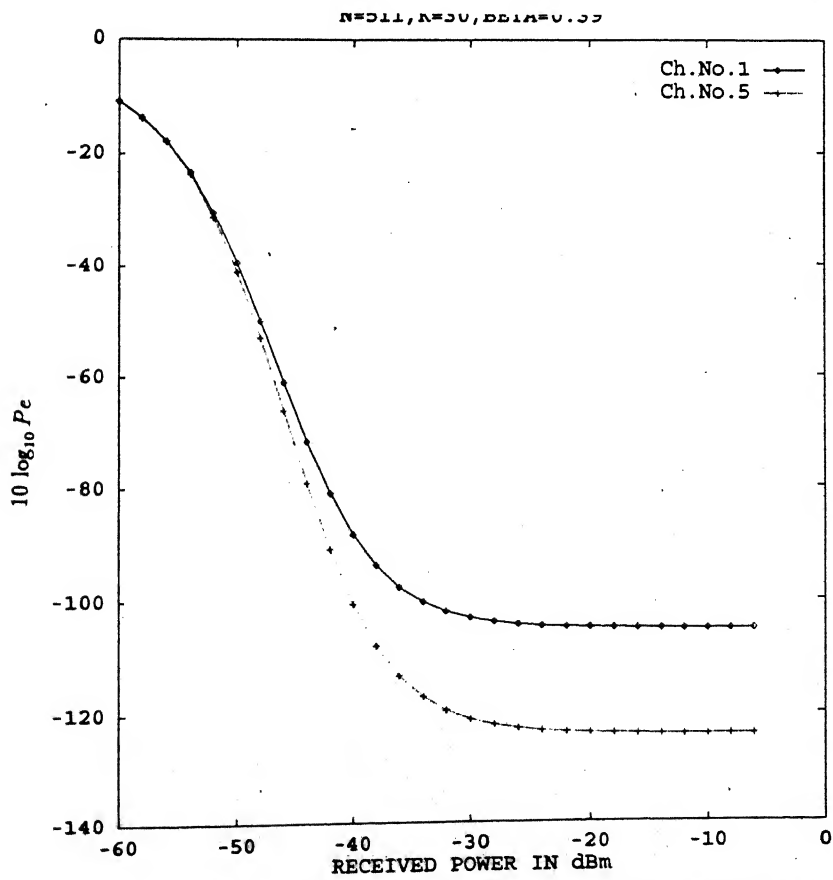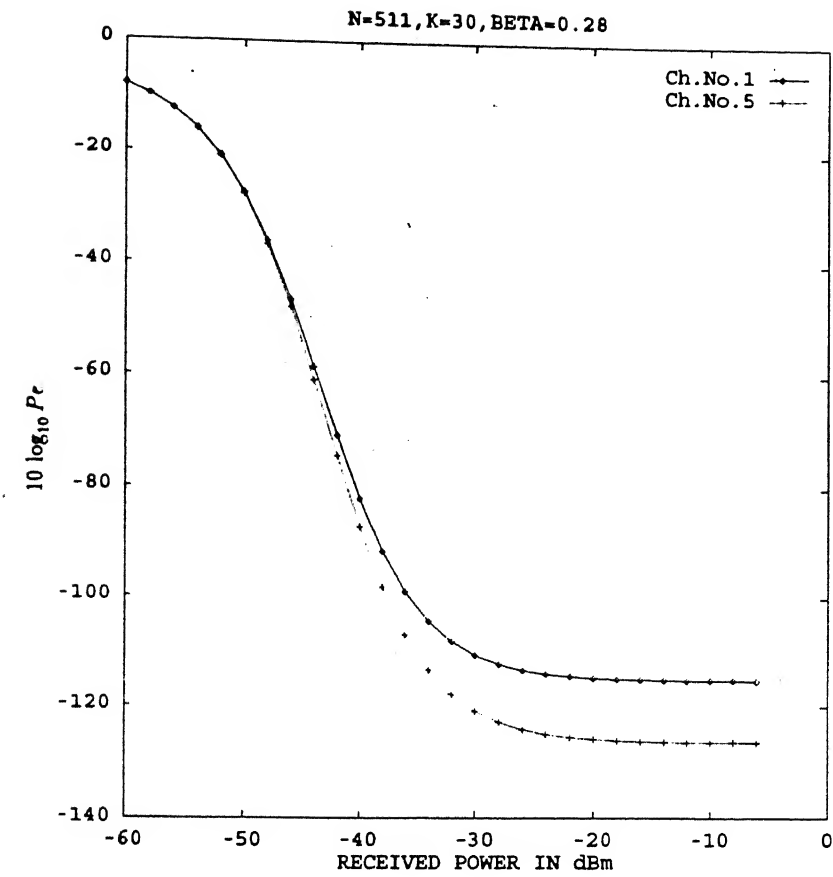Figure 4.20: Probability of Error Vs. Received Power for N=511, k = 20 and 2-18 GHz band

Figure 4.21: Probability of Error Vs. Received Power for N=511, k = 30 and 2-18 GHz band
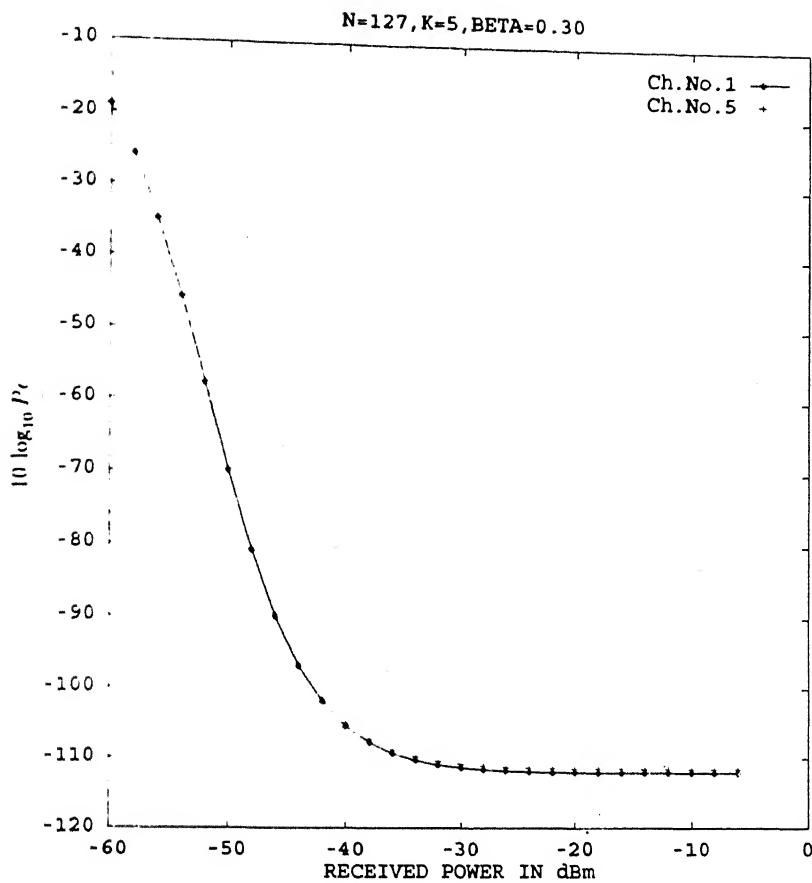
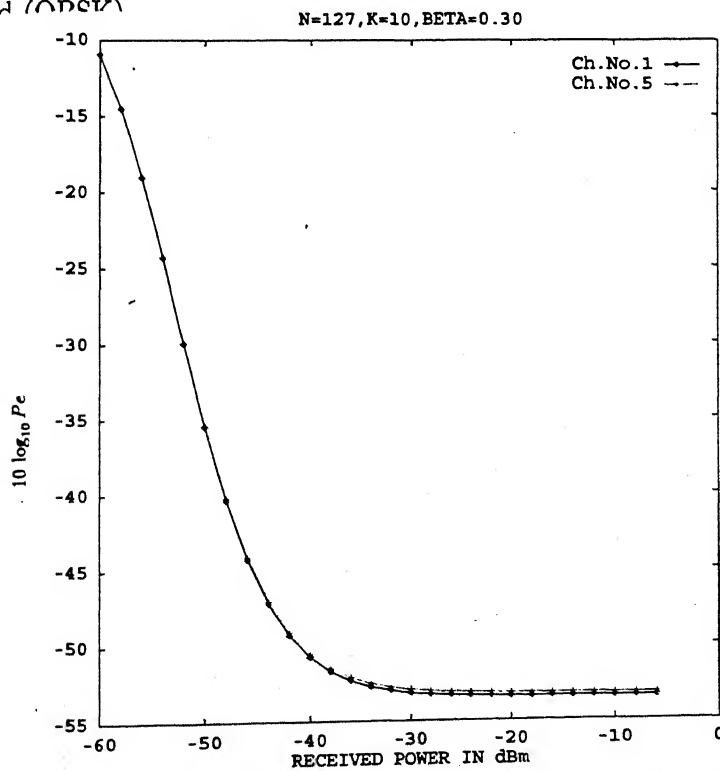Figure 4.22: Probability of Error Vs. Received Power for N=127, k = 5 and 2-4 GHz band (QPSK)

Figure 4.23: Probability of Error Vs. Received Power for N=127, k = 10 and 2-4 GHz band (QPSK)
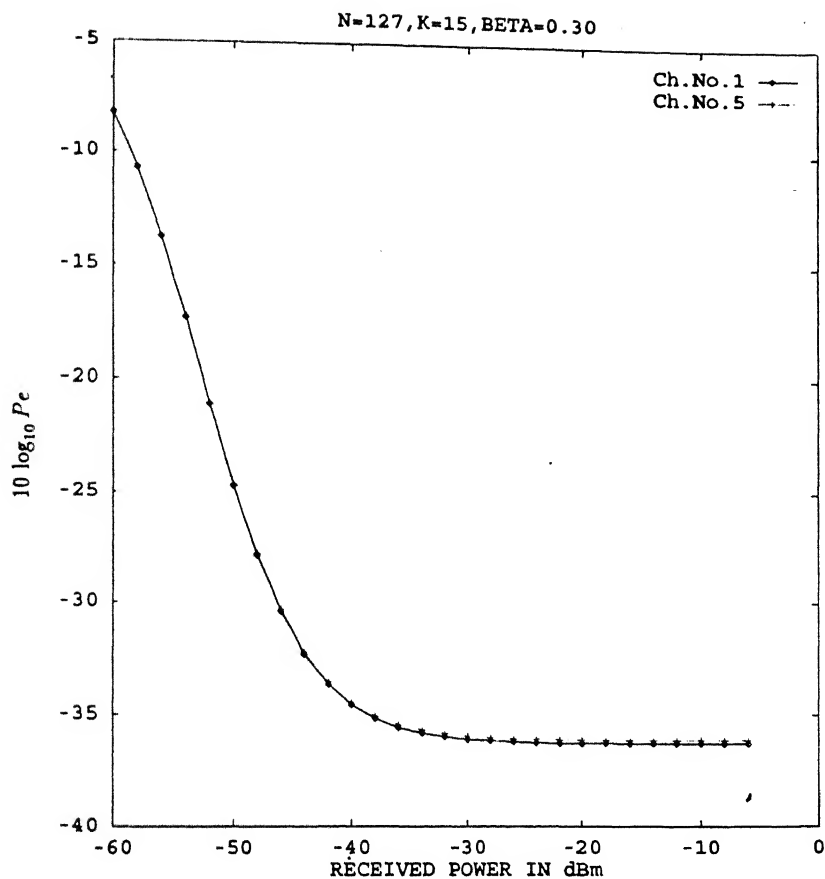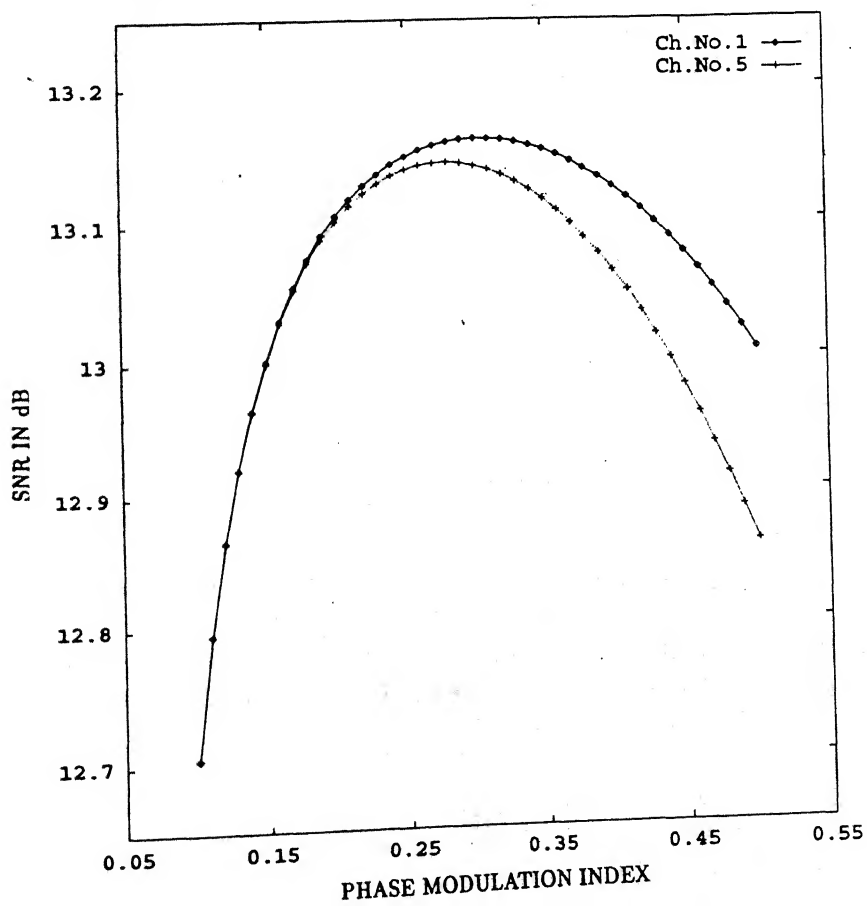
Figure 4.24: Probability of Error Vs. Received Power for N=127, k = 15 and 2-4 GHz (QPSK)

Chapter 5

Direct-Detection CDMA/SCM/WDM Fiber Optic System

In a direct-detection (noncoherent) system the detector responds to the changes in the intensity level of the optical carrier, but, ignores its phase information. Although coherent detection, discussed in the previous chapter, has inherent advantage of having improved sensitivity over direct detection, owing to some practical constraints such as unavailability of narrow linewidth lasers, and good polarization-state control devices, and difficulty in obtaining a coherent local-oscillator output, the widescale deployment of coherent technique is difficult. Therefore, being easier to implement with the available optical components, intensity-modulation (IM) of the optical source and direct-detection (DD) at the receiver is the only alternative. In this chapter an analysis of the CDMA/SCM/WDM fiber optic system using direct-detection at the receiver is presented. Signal-to-noise ratio and probability of error at the receiver output are calculated.

5.1   System Description And Analysis

Overall system model used is the same as shown in Fig. 4.1 for coherent case with two differences. At the transmitter of the coherent system an external optical modulator provides phase-modulation of the optical carrier by the information signal, whereas in the case of direct-detection system the electrical signal directly intensity-modulates the light source and the instantaneous intensity of the optical carrier is proportional to the instantaneous amplitude of the modulating signal current. In heterodyne detection the receiver operates by adding a locally generated optical field to the received optical field, prior to photodetection. In the case of direct-detection, at the receiver the incoming optical signal is converted directly into a demodulated electrical current. This directly detected current is proportional to the intensity of the optical signal.

At the receiver, the photocurrent generated by the optical signal is

$$i(t) = RP_c[1 + \mu s(t)]$$
(5.1)

where,

R is the detector responsivity,
μ is the intensity modulation-index,
P_c the average received unmodulated optical carrier power,
s(t) is the modulating signal which is given by

$$s(t) = \sum_{i=1}^{L} \sum_{k=1}^{K} c_k d_{ik} \cos[\omega_i t + \theta_{ik}]$$
(5.2)

where c_k, d_{ik}, ω_i and θ_{ik} carry the same meaning as given in chapter 4. At the output of the detector, the power in the kth component of the ith subcarrier is

$$P_{ik} = \frac{1}{2K}(R\mu P_s)^2$$
(5.3)

where P_s is the average power of one of the subcarriers.

The total noise in the system is composed of thermal noise, multiple- access interference and intermodulation noise. Since p-i-n photodiode is being used, the shot noise is negligible.

The carrier-to-intermodulation noise ratio at the ith carrier is given by [9].

$$\left(\frac{P}{IM}\right)_i = \frac{S_1^2}{K_2 S_{11}^2 + K_3 S_{111}^2}$$
(5.4)

where,

K_2 = number of second-order IMPs falling in the ith channel,
K_3 = number of third-order IMPs falling in the ith channel,
S_{11} and S_{111} are the amplitudes of the corresponding IMPs, respectively, and
S_1 is the amplitude of the subcarrier at frequency f_i.
S_1, S_{11}, and S_{111} are given by

$$S_1 = 2C I_1(\alpha) [I_0(\alpha)]^{N-1}$$
(5.5)
$$S_{11} = 2C [I_1(\alpha)]^2 [I_0(\alpha)]^{N-2}$$
(5.6)
$$S_{111} = 2C [I_1(\alpha)]^3 [I_0(\alpha)]^{N-3}$$
(5.7)

where,

$$C = \frac{J_0 \tau_p}{qV} - \frac{1}{B\tau_s},$$
(5.8)
$$\alpha = \frac{J/J_0}{1 - \frac{qV}{J_0 B\tau_p \tau_s}},$$
(5.9)

$I_m(\alpha)$ is the modified Bessel function of order m,

J = rms modulation current,

J_0 = dc current,

τ_p = photon lifetime,

τ_s = electron lifetime,

B = Einstein coefficient,

V = volume of the active region, and

q = electronic charge.

Using 3.18, the SNR for the direct-detection CDMA/SCM/WDM system can be written as

$$SNR = [\frac{K-1}{3N} + \frac{K\sigma_{th}^2}{2E_b} + \frac{K\sigma_{im}^2}{2E_b}]^{-1} \qquad (5.10)$$

where,

$E_b = P_{ik}T_b$,

N is the length of the PN sequence,

σ_{th}^2 is the varience of the thermal noise at the receiver output given by

$$\sigma_{th}^2 = \frac{2(N.F.)kT}{R_L},$$

σ_{im}^2 is the variance of the intermodulation noise at the receiver output, and

$$\frac{E_b}{\sigma_{im}^2} = (\frac{P}{IM}); \frac{B}{R_b}$$

where R_b is the bit rate.

The probability of error at the receiver output

$$Pe = Q(\sqrt{SNR}).$$

5.2 Results

Now we consider a CDMA/SCM/WDM direct-detection system having N=127, and the microwave band of 2-6 GHz. Plots of the probability of error vs. received optical power are shown in Fig. 5.1 - Fig. 5.2 for different values of modulation indices and the number of users K.

It is seen that the performance of channel 5 is satisfactory, but, the performance of channel 1 (worst channel) is unacceptable. This is due to a large second order intermodulation noise generated in this case. The performance can be improved if the r.f. bandwidth is confined to less than one octave. So the band of 2-6 GHz can not be used with a direct detection system.

Fig. 5.3 and Fig. 5.4 show the plots for the 4 channel single-octave CDMA/SCM/ WDM system with transmission band extending from 2 GHz to 4 GHz. There is considerable improvement in the performance now because only third-order IMPs are
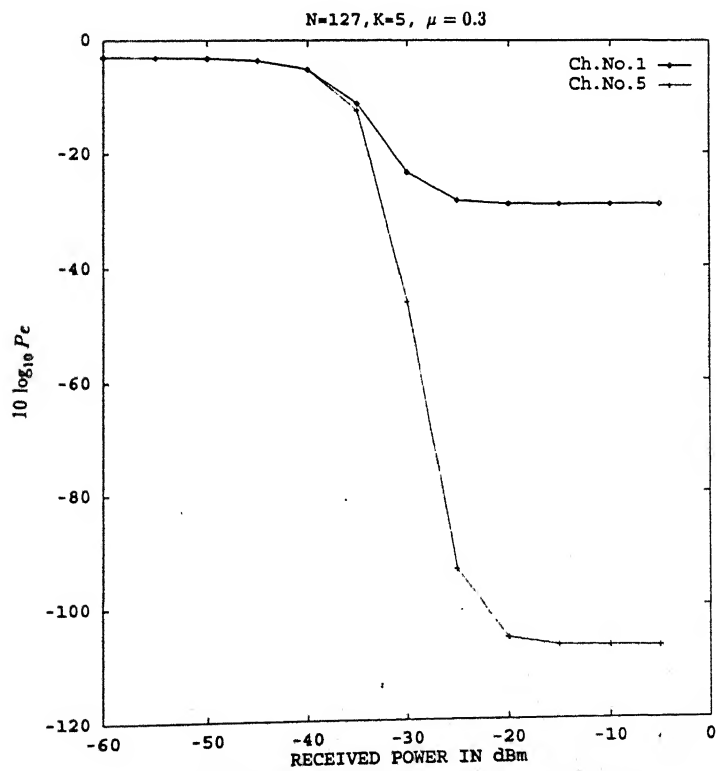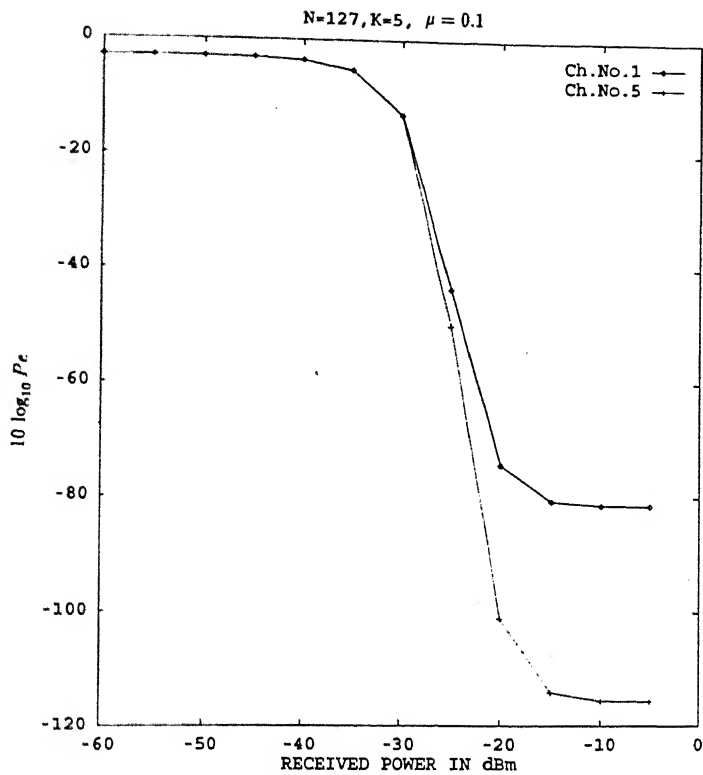
47

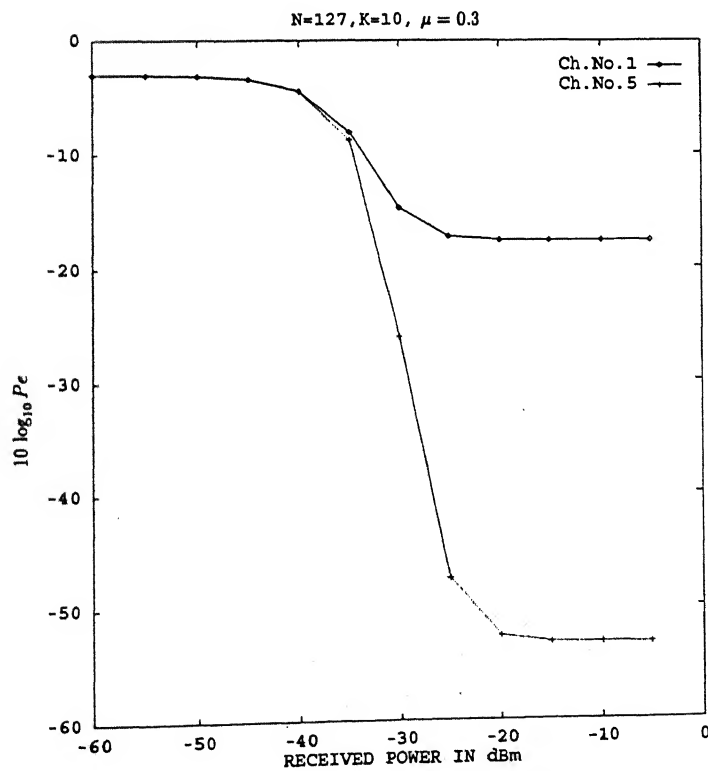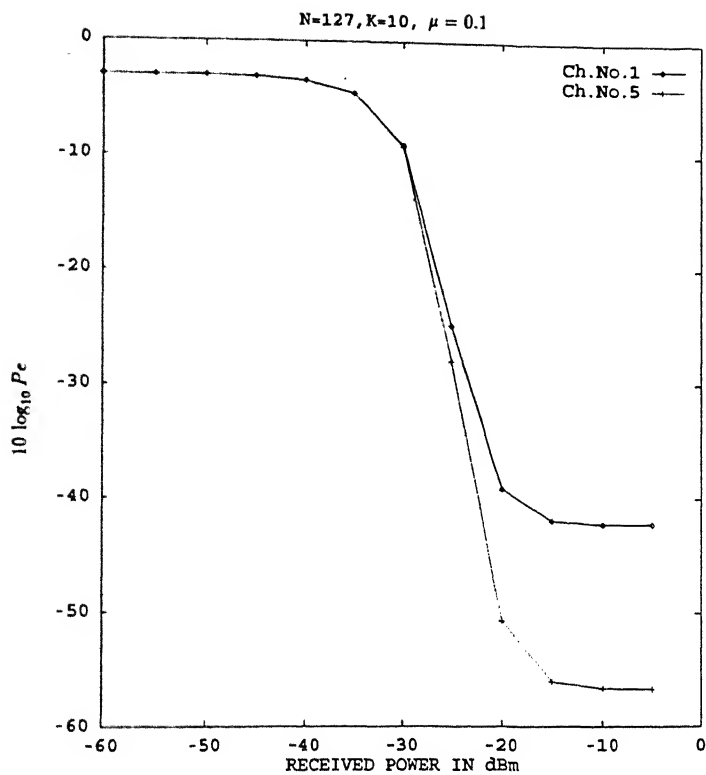Figure 5.1: Probability of Error Vs. Received Power for N = 127, K = 5 and and 2 - 6 Ghz band

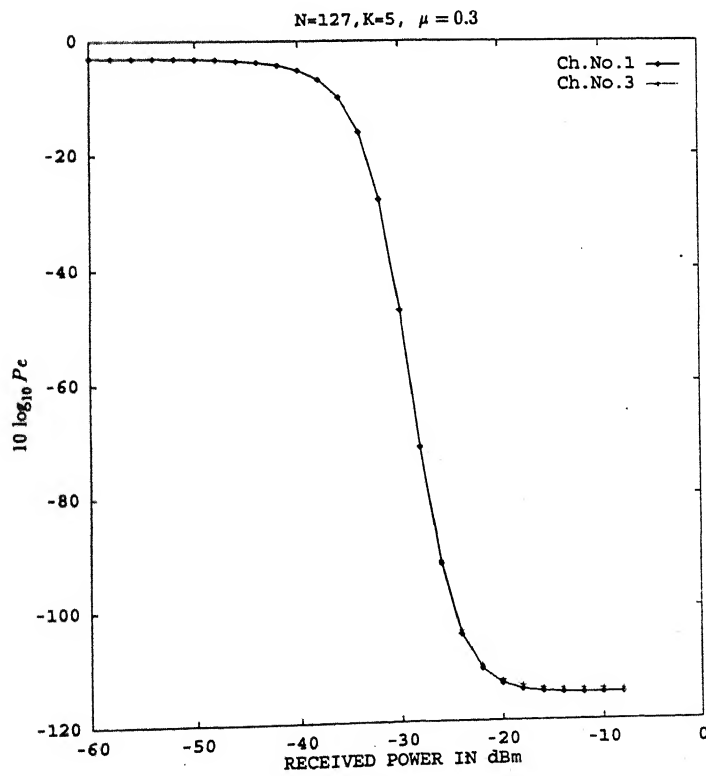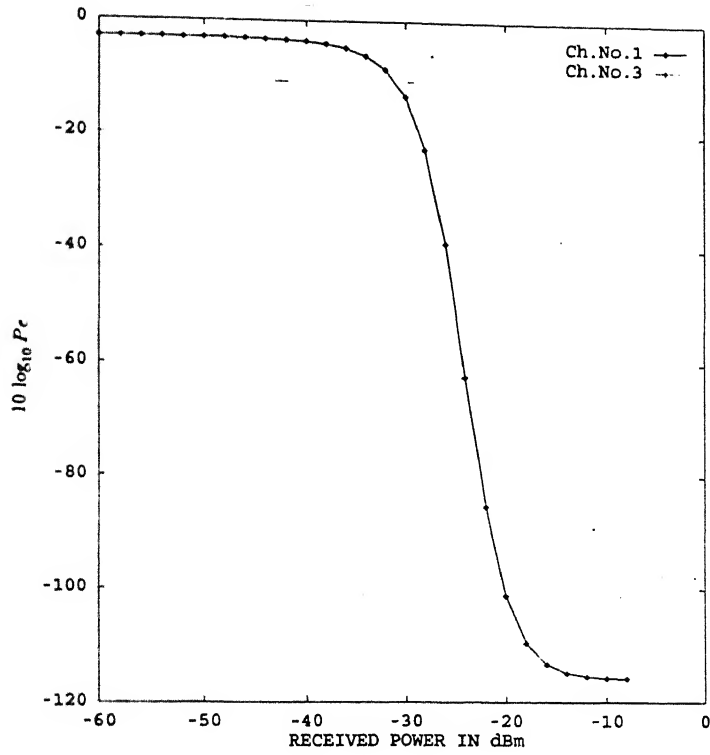Figure 5.2: Probability of Error Vs. Received Power for N = 127, K = 10 and and 2 - 6 Ghz band

Figure 5.3: Probability of Error Vs. Received Power for N = 127, K = 5 and 2 - 4 Ghz band
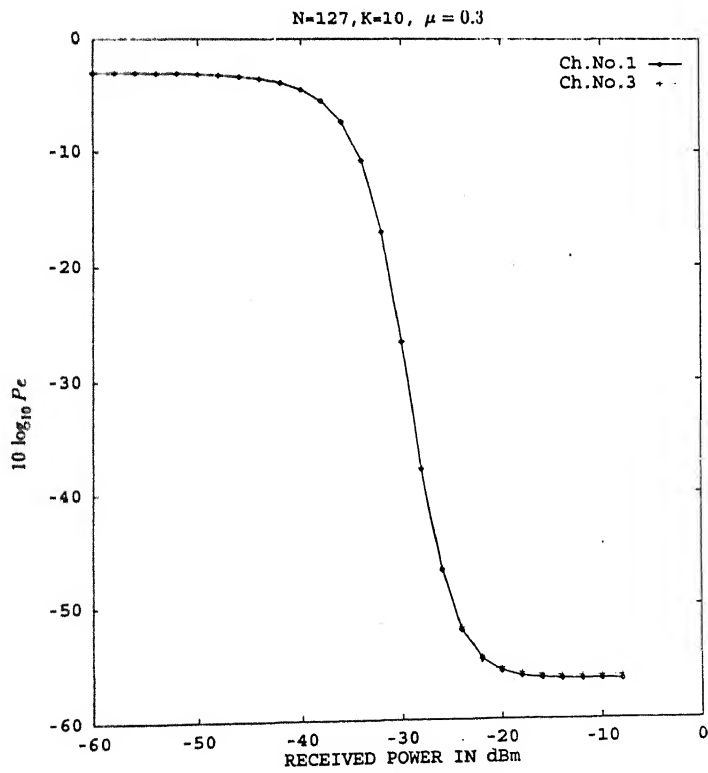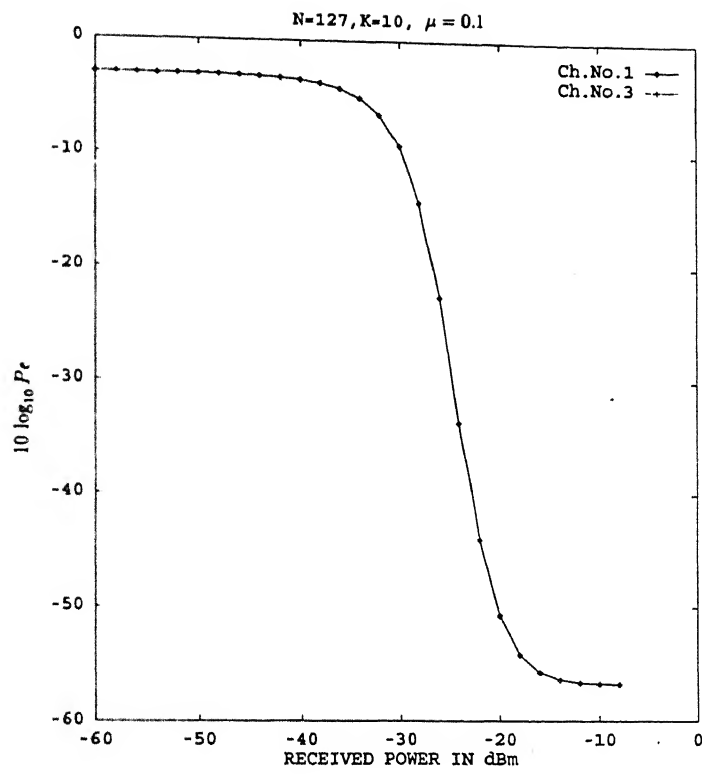
Figure 5.4: Probability of Error Vs. Received Power for N = 127, K = 10 and 2 - 4 Ghz band

present here. The performance of channel 1 is better than that of channel 3 (centre channel) because the centre channel has the most third-order IMPs.

As the modulation index μ increases the performance degrades in the direct detection case unlike in the case of coherent detection where there is an optimum value of β at which the best performance is obtained.

Due to similar reasons as explained in the previous chapter, an error floor has been observed in all the plots.

Chapter 6

28-GHz CDMA/SCM/WDM Systems

Frequency assignment already exists for various services in the 2-6 GHz band considered in the previous chapters. In this band, frequency allocation for L.O.S. communication is typically of the order of 500MHz width. Therefore, the free space part of the system described earlier can not operate in this band. Whereas in the 28-GHz and higher frequency bands frequency allocation for civilian services has not been done as yet. Moreover, components are well developed and are also available freely which work in this frequency band. For this reason, the subcarrier frequencies lying in the 28-GHz band have been chosen in this chapter. The analysis of the CDMA/SCM/WDM system for the frequency band of 26-30 GHz using both coherent as well as direct-detection at the receiver has been done. Since the band is much less than one octave wide, an added advantage is that the second-order intermodulation products can be neglected in this case.

The SNR for the coherent case at the receiver output is given by 4.21, which is reproduced here for convenience

$$SNR = [\frac{K-1}{3N} + \frac{K\sigma_{th}^2}{2E_b} + \frac{K\sigma_{sh}^2}{2E_b} + \frac{K\sigma_{im}^2}{2E_b}]^{-1} \qquad (6.1)$$

where

$$\sigma_{im}^2 = h_3 K_3 R^2 P_{LO} P_s(\frac{\beta^6}{32})$$

The SNR for the direct-detection case is given by

$$SNR = [\frac{K-1}{3N} + \frac{K\sigma_{th}^2}{2E_b} + \frac{K\sigma_{im}^2}{2E_b}]^{-1} \qquad (6.2)$$

Fig. 6.4 and Fig. 6.5 show the plots of the probability of error vs. received power for the coherent case.
Fig. 6.6 and Fig. 6.7 show the same for the direct-detection case.

From the Fig. 6.1 for the coherent case, β_{opt} is calculated to be 0.34 for channel 1 and 0.31 for channel 5. In this case, optimum β for channel 1 is larger because the
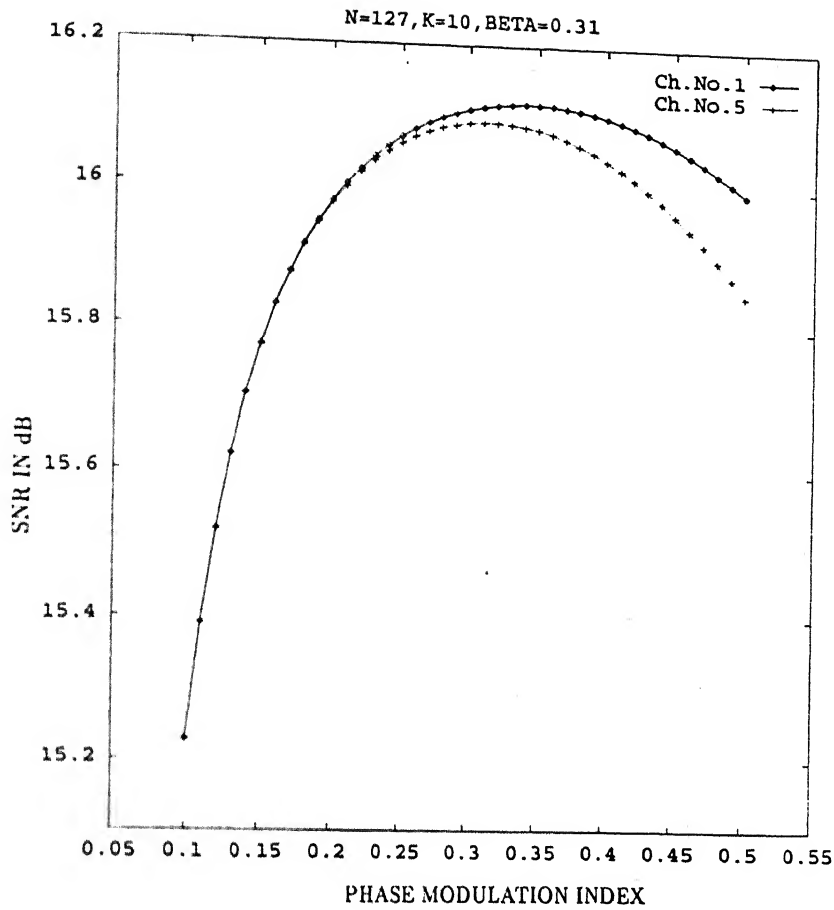
Figure 6.1: SNR vs. Phase Modulation Index for N = 127, K = 5 and 28 Ghz band for Coherent Case

number of second order IMPs is zero and the number of third order IMPs is smaller for channel 1. Due to these reasons performance of channel 1 is seen to be as good as that of channel 5 for both the cases- coherent as well as direct detection.
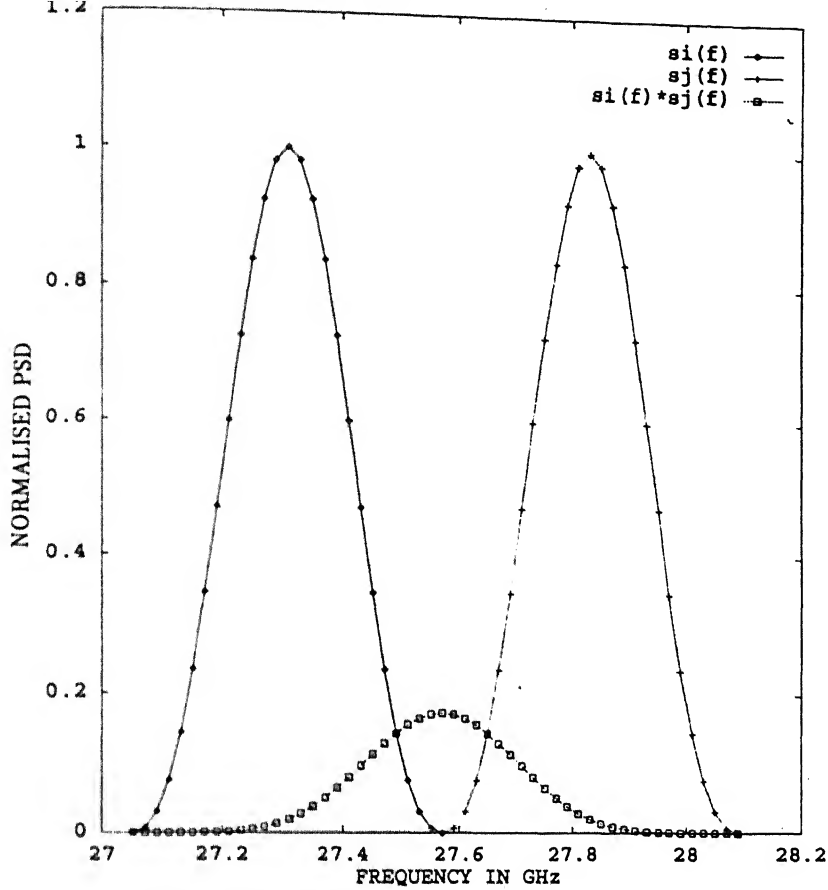
Figure 6.2: Bandpass Spectrum of a Single Second Order IMD Interfering Term (BPSK, N=127 and 26-30 GHz band)
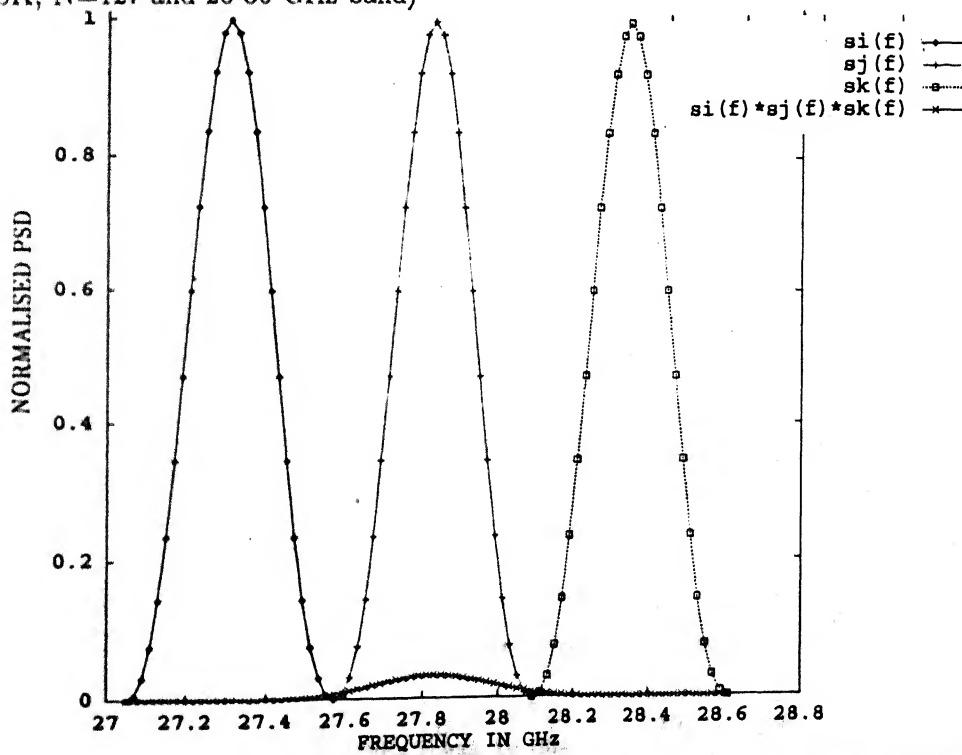
Figure 6.3: Bandpass Spectrum of a Single Third Order IMD Interfering Term (BPSK, N=127 and 26-30 GHz band)
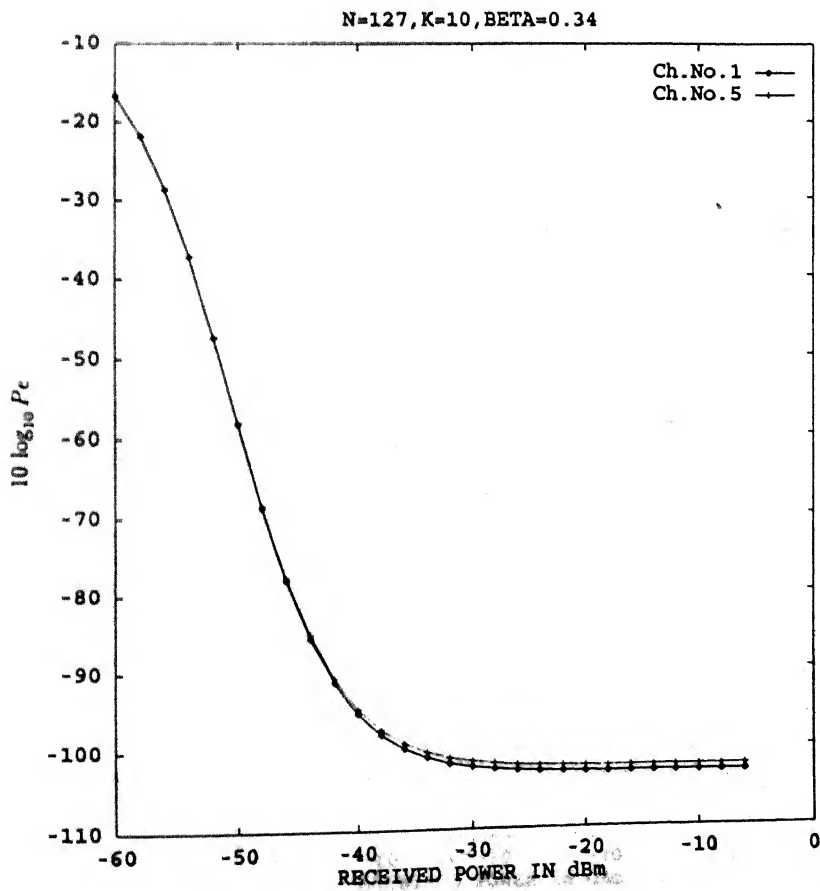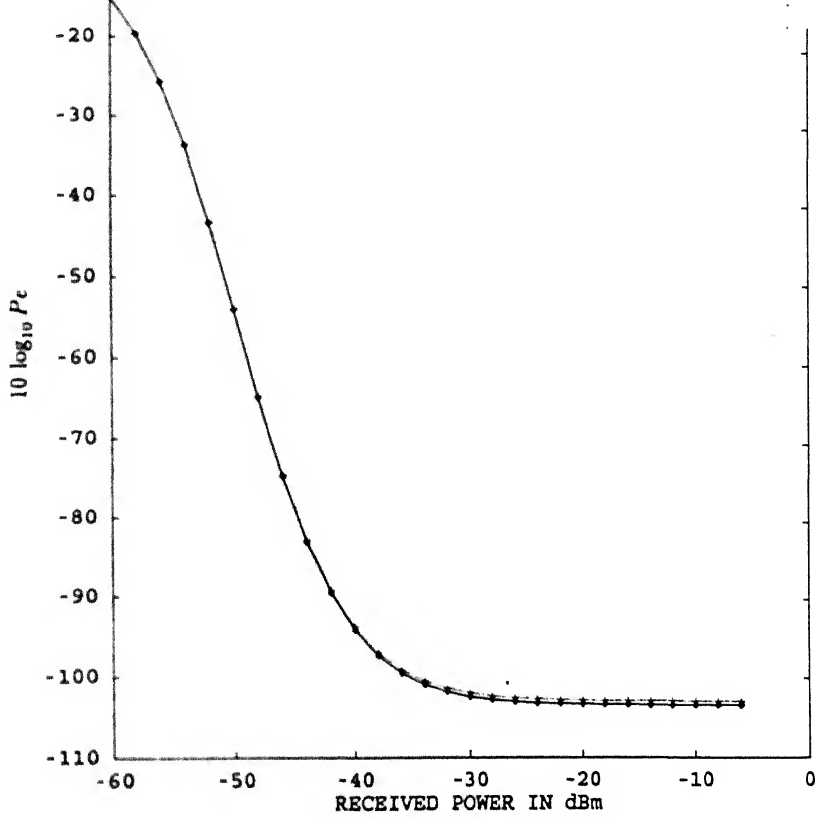
Figure 6.4: Probability of Error Vs. Received Power for N = 127, K = 10 and 28 Ghz band for Coherent Case

Figure 6.5: Probability of Error Vs. Received Power for N = 127, K = 15 and 28 Ghz band for Coherent Case

Figure 6.6: Probability of Error Vs. Received Power for N = 127, K = 5 and 28 Ghz band for Direct Detection Case

Figure 6.7: Probability of Error Vs. Received Power for $N = 127$, $K = 10$ and 28 Ghz band for Direct Detection Case

Chapter 7

Conclusion

In this thesis, a theoretical analysis of a CDMA/SCM/WDM system is given. Different code sequence lengths N have been considered. Depending on 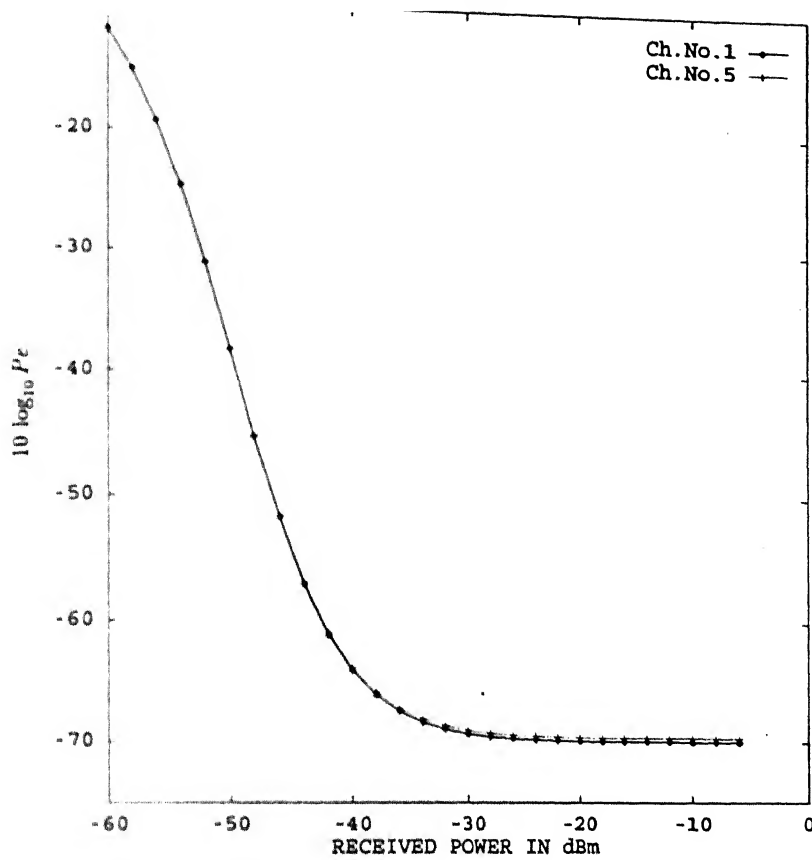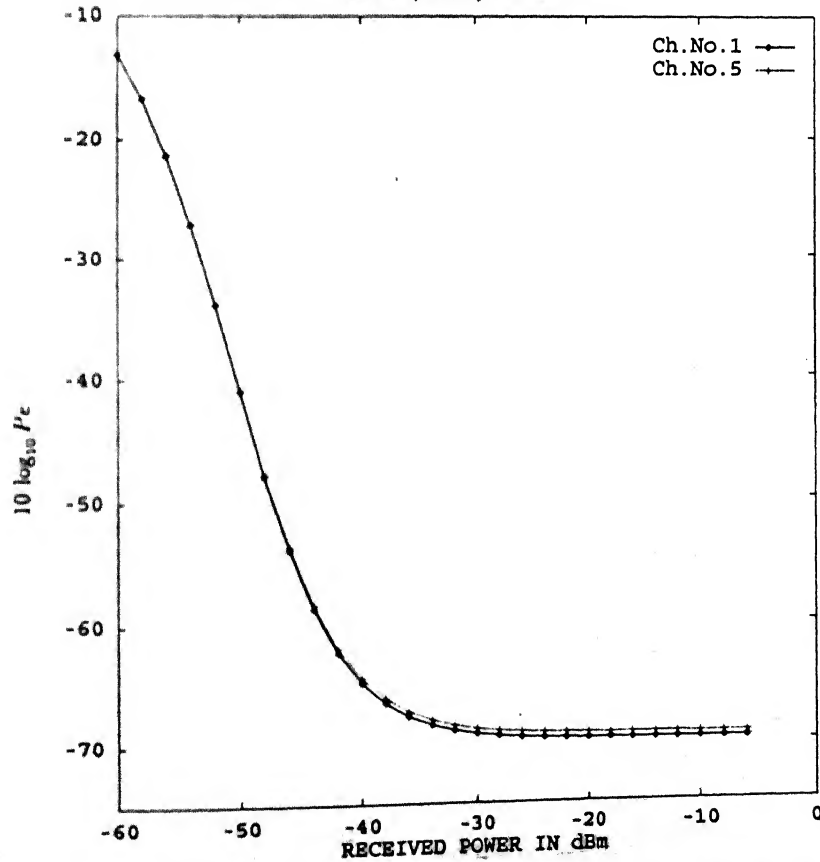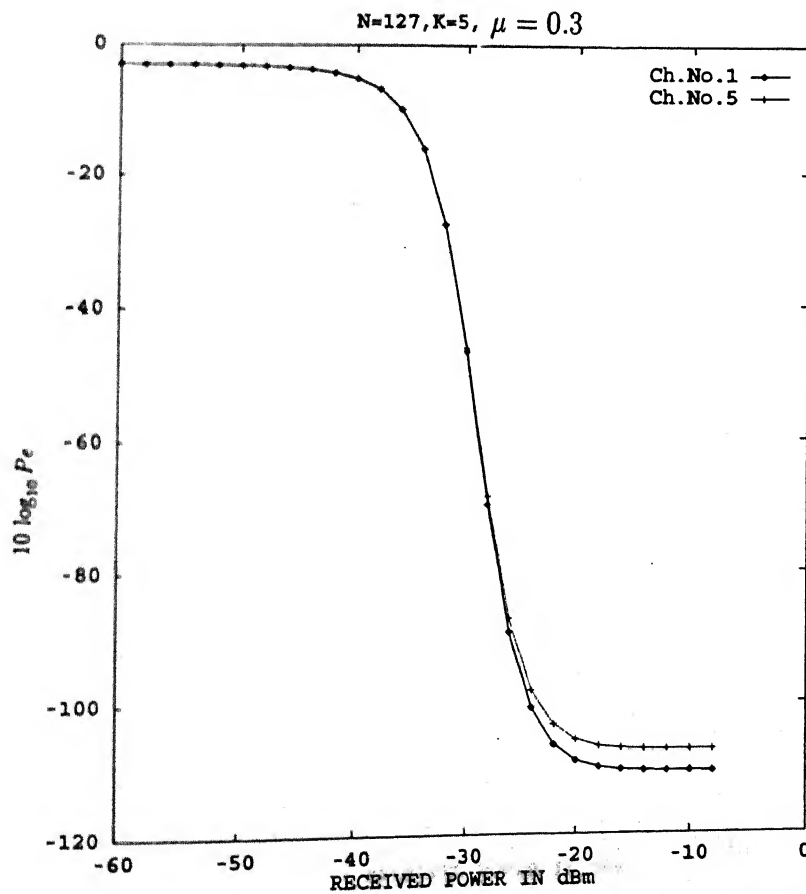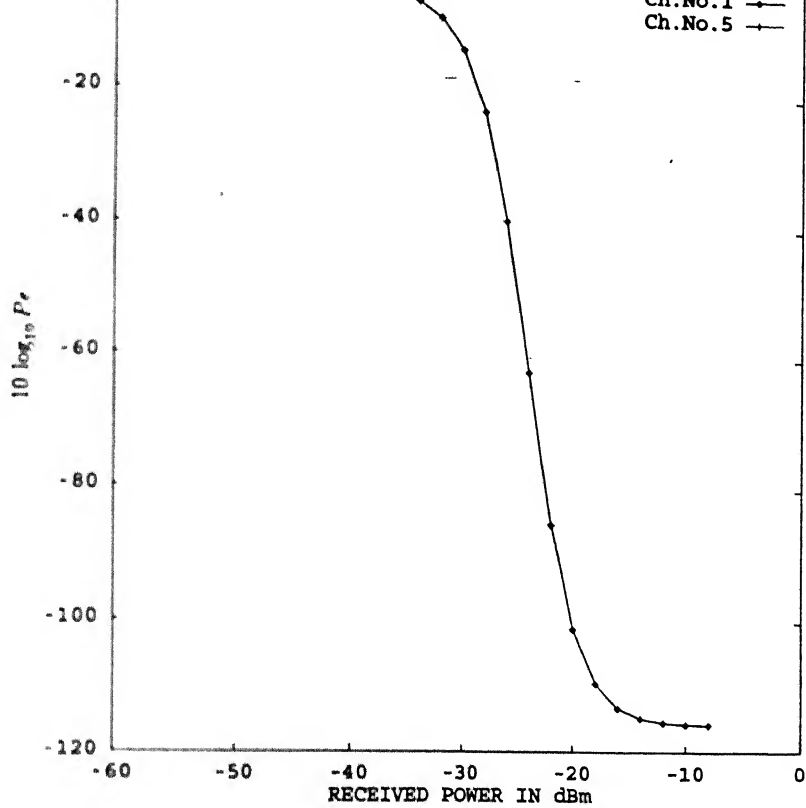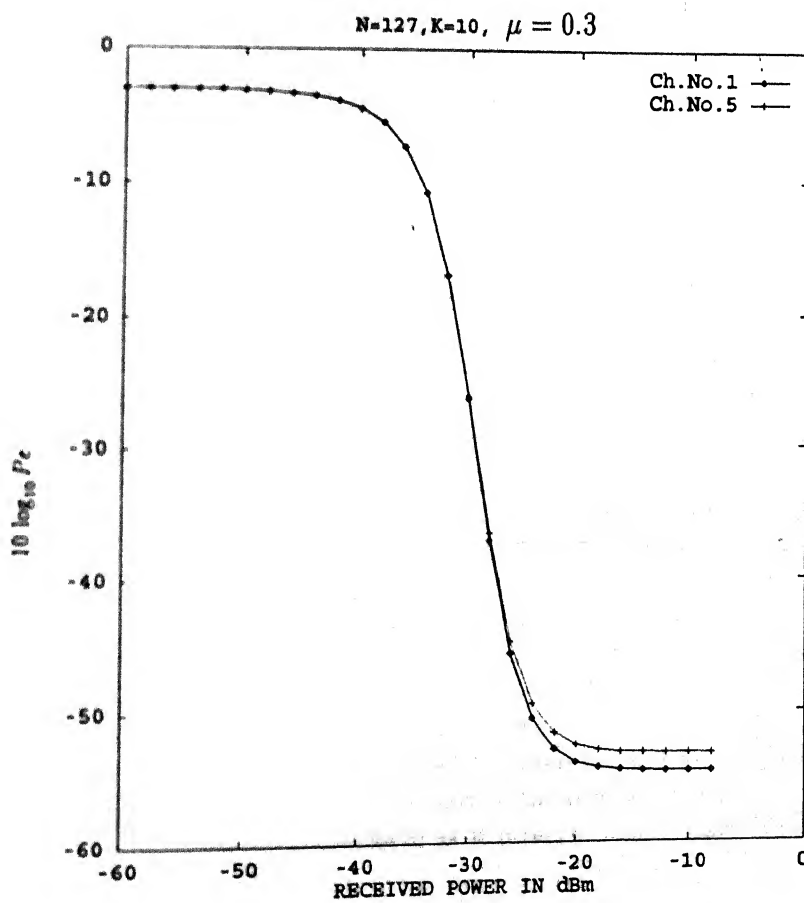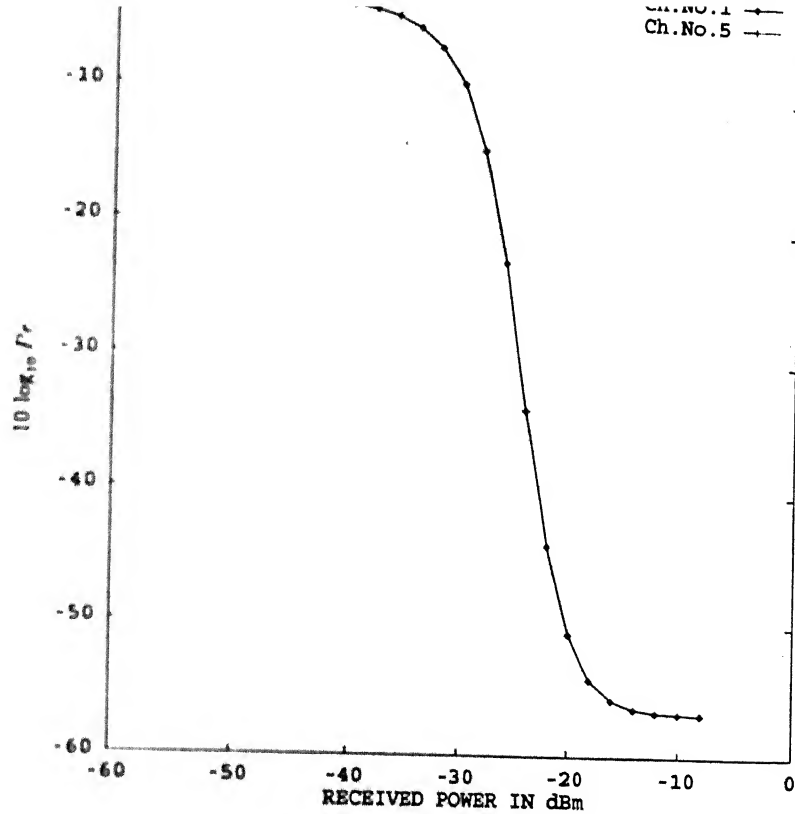the sequence length N and hence, the channel bandwidth, the frequency band in the microwave region is selected accordingly for a multioctave system. Due to nonlinearities in the system, intermodulation distortion occurs. Only second and third order intermodulation products have been considered, since, the distortion caused by all the higher order terms can be assumed to be negligible for all practical purposes. Adjacent channel interference and intersymbol interference are neglected here. The final result includes the effects of thermal noise, shot noise, multiple-access interference and intermodulation noise. Since p-i-n photodiode has been used, shot noise has been neglected for the direct-detection case, but, it has been considered for coherent detection because of large local-oscillator power. Throughout the analysis filter bandwidth is chosen the same as the width of the main spectral lobe.

7.1 Observations

Performance improves considerably as the sequence length N increases as shown in figures. Large N can support more number of users K, but, K is limited by the number of PN sequences having good cross-correlation property. For a fixed N and phase-modulation index β, the probability of error increases with K for the same value of the received power because of increase in both the multiple-access interference as well as the intermodulation noise.

For the coherent case, performance of channel 5 is better than that of channel 1 because contribution due to second order intermodulation products is zero for channel number 5.

For direct detection, the band 2-6 GHz cannot be considered because the performance is not good due to large second order intermodulation distortion. A single-octave band, 2-4 GHz, has been considered in this case, which gives satisfactory performance due to the absence of the second order intermodulation products.

But, since frequency assignment already exists for various services in the 2-6 GHz band, it cannot be used for the free space link part of the overall system. For this reason, the 26-30 GHz band has been considered as at present no allocation exists for

civilian uses in this band. Results have been obtained for both the coherent as well as the direct detection methods in this case. Since the bandwidth here is less than one octave wide, the second order intermodulation products are negligible. Now the performance of channel 1 is better than that of channel 5 due to a smaller number of third order intermodulation products in channel 1 unlike in the previous case. The 28-GHz band can accommodate a larger number of subcarrier channels than used here with acceptable performance as long as the bandwidth remains less than one octave wide.

From the whole analysis it is clear that for the same sequence length N and number of users K, the performance of coherent system is better by about 20 dB than that of the direct detection system.

An error floor is present in all the plots indicating the lower limit on the attainable probability of error. The reason for obtaining the error floor is that for large values of received power, the signal dependent multiple-access interference noise dominates the other noise components present. The error floor for coherent case occurs at lower values of the received power than that for the direct detection case.

Systems with coherent detection in the receiver can support a larger number of channels than that with direct detection, since, the channels can be spaced closer in the former as compared to that in the latter.

If we increase K by keeping $\frac{P_s}{K}$ fixed, intermodulation noise and multiple-access interference increase, and the system performance degrades for the same sequence length N. For example,

for N=127, K=5, $\beta = 0.3$, $\frac{P_s}{K} = -40$ dBm

intermodulation noise = 4.05×10^{-29} watt/hz
multiple-access interference noise = 3.09×10^{-27} watt/hz
SNR = $19.6 dB$, $Pe = 5.2 \times 10^{-22}$

and for N=127, K=10, $\beta = 0.3$, $\frac{P_s}{K} = -40$ dBm

intermodulation noise = 8.1×10^{-29} watt/hz
multiple-access interference noise = 6.9×10^{-27} watt/hz
SNR = $16.1 dB$, $Pe = 6.3 \times 10^{-11}$

If K is increased by keeping P_s fixed, intermodulation noise remains same for both values of K but multiple-access interference noise increases with K for the same sequence length N and the system performance degrades. For example,

for N=127, K = 5, $\beta = 0.3$, $P_s = -30 dBm$

intermodulation noise = 8.1×10^{-29} watt/hz
multiple-access interference noise = 6.1×10^{-27} watt/hz
SNR = 19.6 dB, Pe = 2.87×10^{-22}

and for N=127, K=10, $\beta = 0.3$, $P_s = -30dBm$

$$\text{intermodulation noise} = 8.1 \times 10^{-29} \text{ watt/hz}$$
$$\text{multiple-access interference noise} = 6.9 \times 10^{-27} \text{ watt/hz}$$
$$\text{SNR} = 16.1 \text{ dB, Pe} = 6.3 \times 10^{-11}$$

7.2 Suggestions For Further Work

If the channel spacing is made smaller then the effect of the adjacent channel interference has to be considered. The system performance can be studied under such a situation.

In the 28-GHz band the number of subcarrier channels can be increased to see how the intermodulation distortion affects the system performance.

More bandwidth efficient modulation schemes as continuous phase modulation (CPM) can be used. It is expected that the performance will improve significantly.

Instead of using DS-CDMA, the frequency hopped CDMA scheme can be studied as an alternative.

Appendix

Let the input to nonlinear device be a Gaussian random process x(t). Output will be some function $F\{x(t)\}$ of x(t), denoted by w(t).

Output at instants t_1 and t_2 will be random variables $w(t_1)$ and $w(t_2)$.

$$w(t_1) = F\{x(t_1)\} = F\{x_1\} \text{ i.e., } x(t_1) = x_1$$

$$w(t_2) = F\{x(t_2)\} = F\{x_2\} \text{ i.e., } x(t_2) = x_2$$

The autocorrelation function (ACF) of $w(t)$ is given by

$$\phi_{ww}(t_1, t_2) = E[w(t_1)\, w(t_2)]$$

$$= \frac{1}{2\pi\sqrt{\phi_{11}\phi_{22} - \phi_{12}^2}} \int_{-\infty}^{\infty} dx_1 \int_{-\infty}^{\infty} dx_2\, F\{x_1\}\, F\{x_2\}$$

$$\exp\left[\frac{-1}{2(\phi_{11}\phi_{22} - \phi_{12}^2)}[\phi_{22}x_1^2 - 2\phi_{12}x_1x_2 + \phi_{11}x_2^2]\right]$$

Defining

$$u_1 = \sqrt{\frac{\phi_{22}}{2(\phi_{11}\phi_{22} - \phi_{12}^2)}}\, x_1$$

$$u_2 = \sqrt{\frac{\phi_{11}}{2(\phi_{11}\phi_{22} - \phi_{12}^2)}}\, x_2$$

and

$$C^2 = \frac{\phi_{12}^2}{\phi_{11}\,\phi_{22}}\phi_{ww}(t_1, t_2)$$

$$= \frac{\sqrt{1 - C^2}}{\pi} \int_{-\infty}^{\infty} du_1 \int_{-\infty}^{\infty} du_2\, e^{-(u_1^2 - 2Cu_1u_2 + u_2^2)}$$

$$F[u_1\sqrt{2\phi_{11}(1 - C^2)}]\, F[u_2\sqrt{2\phi_{22}(1 - C^2)}]$$

Since $C^2 \leq 1$, we may write, for later convenience,

$$C = -\cos\alpha$$

where α is an angle between 0 and π.

For Square Law Device

$$F\{x(t)\} = x^2(t)$$

$$\phi_{ww}(t_1 t_2) = \frac{4}{\pi}\phi 11 \phi 22 (1 - C^2)^{5/2} \int_{-\infty}^{\infty} du_1 \int_{-\infty}^{\infty} du_2\, u_1^2\, u_2^2\, e^{-(u_1^2 - 2Cu_1 u_2 + u_2^2)}$$

Evaluating the double integral over each of the four quadrants separately,

$$\int_{-\infty}^{\infty} du_1 \int_{-\infty}^{\infty} du_2\, u_1^2\, u_2^2\, e^{-(u_1^2 - 2Cu_1 u_2 + u_2^2)}$$

$$= 2 \int_{0}^{\infty} du_1 \int_{0}^{\infty} du_2\, u_1^2\, u_2^2\, e^{-(u_1^2 - 2Cu_1 u_2 + u_2^2)}$$

$$= 2\left[I_{22}(\alpha) + I_{22}(\pi - \alpha)\right]$$

where

$$I_{mn}(\alpha) = 2 \int_{0}^{\infty} du_1 \int_{0}^{\infty} du_2\, u_1^m\, u_2^n\, e^{-(u_1^2 + u_2^2 + 2u_1 u_2 \cos \alpha)}$$

From symmetry

$$I_{mn}(\alpha) = I_{nm}(\alpha)$$

and also

$$\frac{dI_{mn}}{d\alpha} = 2\sin \alpha\, I_{m+1,n+1}(\alpha)$$

Above equations are useful for solving the integrals. So we obtain

$$I_{22}(\alpha) + I_{22}(\pi - \alpha) = \frac{\csc^3 \alpha}{8}\left[\pi(3\csc^2 \alpha - 2)\right]$$

$$\phi_{ww}(t_1, t_2) = \frac{4}{\pi}\phi 11 \phi 22 (1 - C^2)^{5/2}\frac{2\csc^3 \alpha}{8}\pi(3\csc^2 \alpha - 2)$$

$$= \phi_{11}\phi_{22}(1 + 2C^2) \qquad \{\sin \alpha = \sqrt{1 - C^2}\}$$

$$= \phi_{xx}(t_1, t_1)\phi_{xx}(t_2 t_2) + 2\phi_{xx}^2(t_1, t_2)$$

If x(t) is stationary Gaussian process, this can be written as

$$R_2(\tau) = R_1^2(0) + 2R_1^2(\tau)$$

For Cubic Law Device

$$F\{x(t)\} = x^3(t)$$

$$\phi_{ww}(t_1, t_2) = \frac{8}{\pi}\phi_{11}^{\frac{3}{2}}\phi_{22}^{\frac{3}{2}}(1 - C^2)^{\frac{7}{2}}\int_{-\infty}^{\infty} du_1 \int_{-\infty}^{\infty} du_2\, u_1^3\, u_2^3\, e^{-(u_1^2 - 2Cu_1u_2 + u_2^2)}$$

Again evaluating the double integral over each of the four quadrants

$$\int_{-\infty}^{\infty} du_1 \int_{-\infty}^{\infty} du_2\, u_1^3\, u_2^3\, e^{-(u_1^2 - 2Cu_1u_2 + u_2^2)}$$

$$= 2\int_{0}^{\infty} du_1 \int_{0}^{\infty} du_2\, u_1^3\, u_2^3\, e^{-(u_1^2 - 2Cu_1u_2 + u_2^2)}$$

$$= 2[I_{33}(\alpha) - I_{33}(\pi - \alpha)]$$

$$I_{33}(\alpha) - I_{33}(\pi - \alpha) = \frac{\csc^4\alpha}{16}\{6\pi\cot\alpha - 15\pi\csc^2\alpha\cot\alpha\}$$

$$\frac{\csc^4\alpha}{16}\pi\cot\alpha\{6 - 15\csc^2\alpha\}\phi_{ww}(t_1, t_2)$$

$$\frac{8}{\pi}\phi_{11}^{\frac{3}{2}}\phi_{22}^{\frac{3}{2}}(1 - C^2)^{\frac{7}{2}}\cot\alpha\csc^4\alpha[6 - 15\csc^2\alpha]$$

We know $\cot\alpha = -C(1 - C^2)^{-1/2}$

$$\phi_{ww}(t_1, t_2) = \phi_{11}^{\frac{3}{2}}\phi_{22}^{\frac{3}{2}}C[9 + 6C^2] = 9\phi_{12}\phi_{22} + 6\phi_{12}^3$$

For a stationary Gaussian process

$$R_3(\tau) = 9R_1(\tau)R_1^2(0) + 6R_1^3(\tau)$$

References

[1] M. B. Pursley, "Performance evaluation for phase-coded spread-spectrum multiple-access communication-Part 1: System analysis", IEEE Transactions on Communications, vol. COM-25, No. 8, pp. 795-799, August 1977.

[2] F. D. Garber and M. B. Pursley, "Performance of offset quadriphase spread-spectrum multiple-access communications", IEEE Transactions on Communications, vol. COM-29, no. 3, pp. 305-313, March 1981.

[3] E. A. Geraniotis, "Performance of noncoherent DS/SSMA communications", J.S.A.C., vol. SAC-3, no. 5, pp. 687-694, September 1985.

[4] T. E. Darcie, "Subcarrier multiplexing for multiple-access lightwave networks", Journal of Lightwave Technology, LT-5, pp 1103-1110, August 1987.

[5] C. Desam, "Optical interference in lightwave subcarrier multiplexing systems employing multiple optical carriers", Electronics Letters, vol. 24, pp. 50-52, 1988.

[6] C. Desam, "Optical interference in subcarrier multiplexed systems with multiple optical carriers", IEEE J.S.A.C., vol. 8, no. 7, pp. 1290-1295, September 1990.

[7] P. Hill and R. Olshansky, "Twenty channel FSK subcarrier multiplexed optical communication system for video distribution", Electronics Letters, vol. 24, pp. 892-893.

[8] R. Gross and R. Olshansky, "Multichannel coherent FSK experiments using subcarrier multiplexing techniques ", J. Lightwave Technology, vol. 8, pp. 406-415, 1990.

[9] M. T. Abuelma'atti, "Carrier-to-intermodulation performance of multiple FM/FDM carriers through a GaAlAs hetrojunction laser diode", IEEE Transactions on Communications, vol. COM-33, no.3, March 1985.

[10] "Transmission Systems for Communication", Bell Telephone Laboratories, Incorporated, 1970.

[11] N. Madhava Reddy, "Application of continuous phase modulation techniques in coherent subcarrier multiplexing", M. Tech. Thesis, February 1993.

[12] J. Daly, "Fiber optic intermodulation distortion", IEEE Transactions on Communications, vol. COM-30, no. 8, pp. 1954-1958, August 1982.

[13] B. Arnold, "Third order intermodulation products in a CATV system", IEEE Trans. Cable TV, vol. CATV-2, pp. 67-80, April 1977.